WRC Technical Report 0318-01

Black Rock City, Nevada

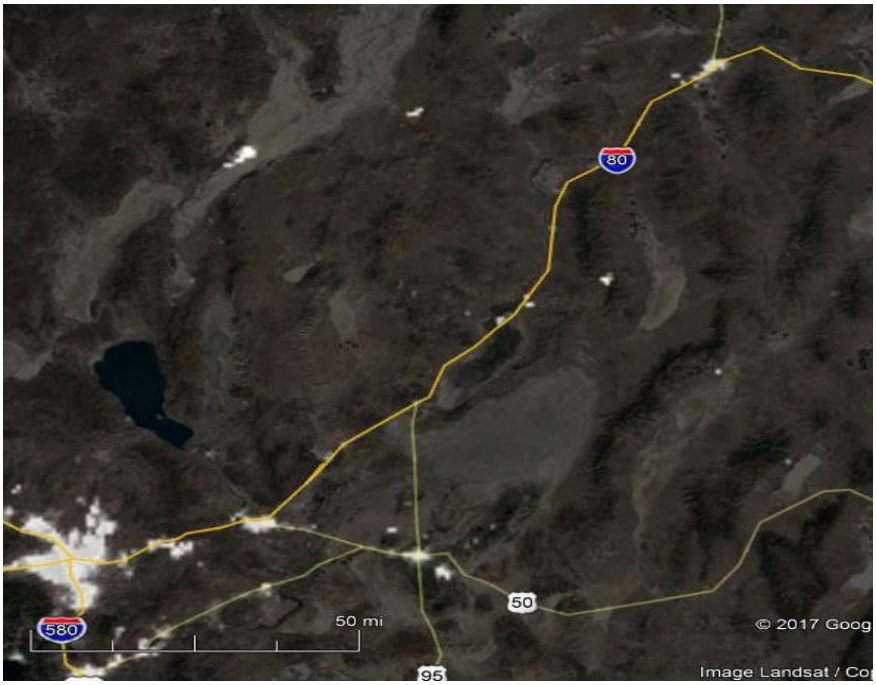

3/15/2018

Artificial Light at Night Assessment

This technical report describes quantitative and qualitative measures of artificial light at night (ALAN) associated with Black Rock City, Nevada during and around the annual Burning Man event.

Prepared by

Western Research Company, Inc. (Tucson, Arizona)

Authors: Dr. Eric R. Craine and Dr. Brian L. Craine

Table of Contents

Abbreviations

ALAN	Artificial light at night
BLM	Bureau of Land Management
DNB	Day night imaging band
ESRI	Environmental Systems Research Institute, Inc.
GeoTIFF	TIFF format images that include geo-position information
HDF5	Data file format for distributing satellite data
LANI	Light at night index
NPS	National Park Service
mi	Statute mile
NOAA	National Oceanic and Atmospheric Administration
NPP	National Polar-Orbiting Partnership
r^2	Coefficient of determination
SED	Spectral energy distribution
sr	Steradian
SQM-L	Sky quality meter
UL	95% confidence upper limits
VIIRS	Visible Infrared Imaging Radiometer Suite Sensor
VCM	Satellite images excluding any data impacted by stray light.
W	Watts
WRC	Western Research Company, Inc (Tucson, AZ)

List of Figures

List of Tables

Black Rock City, Nevada

ARTIFICIAL LIGHT AT NIGHT ASSESSMENT

Abstract

This report describes results of a satellite data survey and ground-based survey to characterize artificial light at night (ALAN) associated with the Burning Man event held annually at Black Rock City, NV. Principal conclusions of the study are that 1) the average nightly radiance per night during the event has increased modestly over the last 5 years, 2) the average nightly radiance during the event is quite favorable compared to other cities in Nevada, 3) the rate of increase in radiance per person occurs for the first ~20,000 people suggesting that increasing the number attendees would have a relatively small impact upon further increases in radiance, and 4) there is a significant amount of ALAN that is not optimally shielded and is misdirected above the horizon. The average nightly radiance is increasing with time; however, accurate predictive models will require that the 2017 baseline be followed by a few years of additional measurements to verify the current trend. In spite of the special nature of the Burning Man event there are ALAN mitigation strategies that could significantly improve the environmental impact of the event lighting. The ground-based protocol of the 2011 event can, and should, be significantly improved for future evaluation of the event-associated ALAN environment.

1. Introduction

This is the Final Report submitted by Western Research Company, Inc. of Tucson, Arizona to Environmental Management and Planning Solutions, Inc. (EMPSi) of Reno, Nevada in fulfillment of the contract “Burning Man Event Special Recreation Permit”, EMPSi Job # C-6077/sub-contract 001 dated 8/25/2017 (hereafter “Contract”). This report is accompanied by a supplemental flash drive the contents of which are listed in appendix A.

2. Background

2.1 Nature of the Burning Man Event

Burning Man is organized by the Burning Man Project, a non-profit organization that, in 2014, succeeded a for-profit limited liability company (Black Rock City, LLC) that was formed in 1997 to represent the event's organizers, and is now considered a subsidiary of the non-profit organization. Burning Man is an annual gathering in a temporary community, Black Rock City, erected in the Black Rock Desert of northwest Nevada. The late summer event is described as an experiment in community and art, adhering to ten main principles: "radical" inclusion, self-reliance, and self-expression, as well as community

cooperation, civic responsibility, gifting, de-commodification, participation, immediacy, and leaving no trace.

Black Rock City is constructed and dismantled each year. The construction generally begins around the first week of August and dismantling occurs within a few weeks of the ending of the festival. The event is notable for large interactive artworks and a variety of special vehicles (mutant vehicles). Currently the population of Black Rock City swells to as many as about 80,000 people with an average of about 65,000 during the typically eight day event. Significant amounts of night lighting may be employed during the construction and to a lesser degree the dismantling of the city.

Black Rock City and the Burning Man event operate under control of the Bureau of Land Management which provides a Special Recreation Permission Stipulations document detailing event parameters [1].

2.2 Local Environment

Black Rock City is a transient city and home for the Burning Man event located in the Black Rock desert about 10 miles from the small community of Gerlach. The Black Rock Desert, in the far northwest of Nevada, was once covered by the ancient Lake Lahontan, most of which is now just a series of dry, alkaline flats. The most level and uniform section is the Black Rock Playa, which stretches for 35 miles, beginning just south of the small town of Gerlach and extending northeast towards the edge of the Black Rock Range - a region completely dry much of the year. The desert is managed by the Bureau of Land Management (BLM) as a National Conservation Area with regulated, multi-use recreation.

Figure 2.1. View over the Black Rock desert.

2.3 Importance of Artificial Light at Night

Large scale artificial light at night (ALAN) is a relatively new phenomenon in the history of man but has quickly become ubiquitous. It serves important roles in expanding the scope and scale of human activity and is a critical component allowing for the safe conduct of activities at night. ALAN can have some positive impacts on human health, such as relief for seasonal depression. However, it is becoming increasingly accepted that ALAN has negative impacts upon 1) the ecosystem, 2) human health, and 3) observation of the night sky (both by professional astronomers and the lay public).

There are competing and conflicting impacts of ALAN, but everyone benefits from minimizing the levels of unnecessary ALAN (and consequent energy conservation) in the context of local activities[2]. To accomplish this goal it is important to measure, analyze and monitor the levels of ALAN objectively to understand the need for, and types of, mitigation that may be productive.

2.4 The Goal of this Project

This project was intended to characterize ALAN contributions from the Burning Man event using two techniques: 1) quantitative nighttime satellite imaging, and 2) replication of a protocol used at the 2011 Burning Man event (Appendix B, hereafter the "2011 Protocol"). The goal was to understand temporal changes in Burning Man-related ALAN and to predict future impacts of increases in event attendance.

The satellite data were used to evaluate ALAN both during and outside the event dates, and to look at ALAN evolution as a function of time, encompassing multiple years of events. The 2011 Protocol replication was requested by the client as a way of comparing one past event with the 2017 event. Unfortunately, the 2011 Protocol is of rather limited utility (see Appendix C).

The satellite data allowed construction of models that can be used predictively to help characterize the impact of future events. The impact of population levels at Black Rock City was of particular interest.

A final goal of the project was to suggest future monitoring methods that can help resolve the conflict between different models, and to significantly improve the understanding of environmental impacts of the event lighting.

3. Methods and Data Collection

3.1 Satellite ALAN Analysis

3.1.1 Nightly Satellite Data

The Suomi NPP satellite [3] images the Black Rock City area on a nightly basis, providing a useful resource for monitoring upward radiating light levels. Nighttime imaging is provided by a scanning radiometer on the Suomi satellite called the Visible Infrared Imaging Radiometer Suite (VIIRS). To measure the artificial light at night component it is preferable to obtain imaging in the absence of moonlight and the absence of interfering cloud cover or severe atmospheric conditions (e.g. heavy dust storms).

The first criterion of absent moonlight can be achieved by using satellite measurements obtained when the lunar zenith angle is greater than or equal to 110^0 (i.e. the moon is at least 20^0 below the horizon).

However, the extreme time constraints imposed by evaluating the ALAN associated with the Burning Man Event (a narrow window of about a week) prompted us to employ corrections to the data to remove the influence of direct moonlight (see Figure 3.1). This was possible since most of the year there is no discernible ALAN present at the Black Rock City site, allowing the measurement of the relative reflectance of the site compared to a nearby uninhabited, but geologically similar, portion of the playa. This control playa site (see Figure 3.3) can serve to provide a measure of the nightly moonlight component which can be subtracted from measurements obtained at the Black Rock City site (see Figure 3.3). This correction factor allows us to expand the number of nights with usable data.

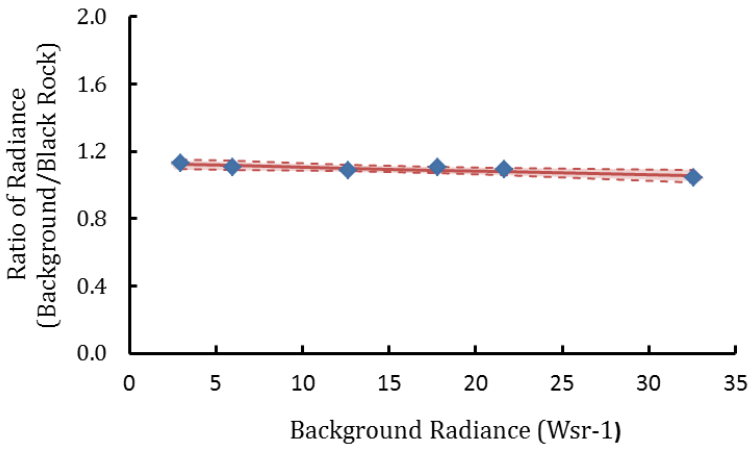

Figure 3.1. Ratio of Playa background control to Black Rock City.
The ratio of the radiance of the control site to the Black Rock City site, in the absence of ALAN (June of 2016), is displayed over a range of radiances due to reflection of moonlight. Measured nights are shown as blue diamonds with a solid red fit. The dashed line and shaded area is the 95% confidence interval. The average ratio over a broad range is 1.09 (standard deviation of 0.026).

The second criterion of cloud screening is based on the spectral analysis of the VIIRS sensor data using cloud identification algorithms developed by NASA [4]. The NASA analysis characterizes the cloud status over each pixel in the satellite image using a four point confidence scale (0-3) regarding cloud-free status. A score of 0 indicates a 100% confidence of a cloud free pixel. A score of 1 is 50-99% confidence, a score 2 is 1-49% confident and a score of 3 is 100% confident of cloud cover. The Suomiutils™ software

(Western Research Company, Inc., Tucson, AZ) calculates values (C_1 through C_4) which are the sum of the number of pixels in an area with the corresponding cloud score (0 through 3). The software uses these values to calculate a cloud index (CI) for each identified area in the image (e.g. Black Rock City area):

$$CI = 1 - \left(\frac{C_1}{C_1 + C_2 + C_3 + C_4}\right)$$

The CI index varies from 0 to 1, with 0 being highest confidence of cloudless pixels and 1 being the highest confidence of cloud interference. For this project we have used only images that have a CI ≤ 0.1 over an area of interest.

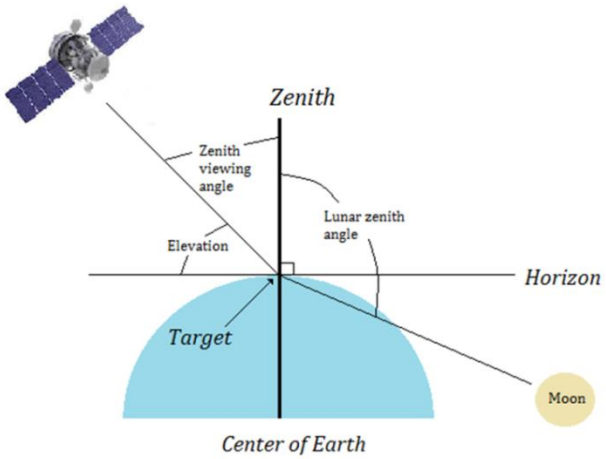

Figure 3.2. Illustration of zenith angle and elevation definition.
Lunar angle of 120^0 puts the moon well below horizon.

Raw satellite HDF5 data files (including radiance files, geo position files, and the VIIRS Cloud Mask Intermediate product) for nights around the time of the Burning Man event during the years 2012-2017 were downloaded from the CLASS system [5] . The nightly files are processed using the Suomiutils™ software package. Suomiutils™ opens the HDF5 data file and ESRI shapefiles from which it can extract sum radiance, average radiance, satellite zenith angle, satellite azimuth angle, lunar zenith angle, and calculate the cloud index for geo-locations specified by the shapefile (see Figure 3.2). This preliminary analysis allows for the determination of the above listed suitability criteria. The nighttime observations fulfilling the criteria are listed in Appendix E.

The accepted data files (radiance and corresponding geo position files) were segmented to a rectangular region encompassing Black Rock City and surrounding area in northern Nevada (coordinates: Upper Left (119d27'21.05"W, 41d29' 8.15"N); Lower Left (119d27'21.05"W, 39d38'25.94"N); Upper Right (117d33'17.12"W, 41d29' 8.15"N); Lower Right (117d33'17.12"W, 39d38'25.94"N). The data were converted to GeoTIFF format images with pixel size of 461x393 meters to match the NOAA monthly composite format for further analysis. The original radiance values (R_0) are floating point numbers with units of Watts/cm^2/sr. During conversion to GeoTIFF format the radiance is converted to a 16-bit

format data number (dn) linearly related to the original radiance. The conversion is accomplished as:

$$dn = \frac{R_0(Max_o - Min_o)}{(Max_i - Min_i)} + b$$

Where Max_o is the maximum dn (65535 for 16-bit image) and Min_o is the minimum dn or 0. Max_i is the maximum radiance value to be measured (6×10^{-7} $Wcm^{-2}sr^{-1}$) and Min_i is the minimum radiance value (10^{-11} or ~0 $Wcm^{-2}sr^{-1}$). The intercept, b, is 0. The radiance values measured from the 16-bit GeoTIFF images are recovered by reversing this process to calculate the R_o from the measured dn. The area dependence is removed by multiplying the value by the known area imaged by the satellite to obtain units of Wsr^{-1} for the comparison of results.

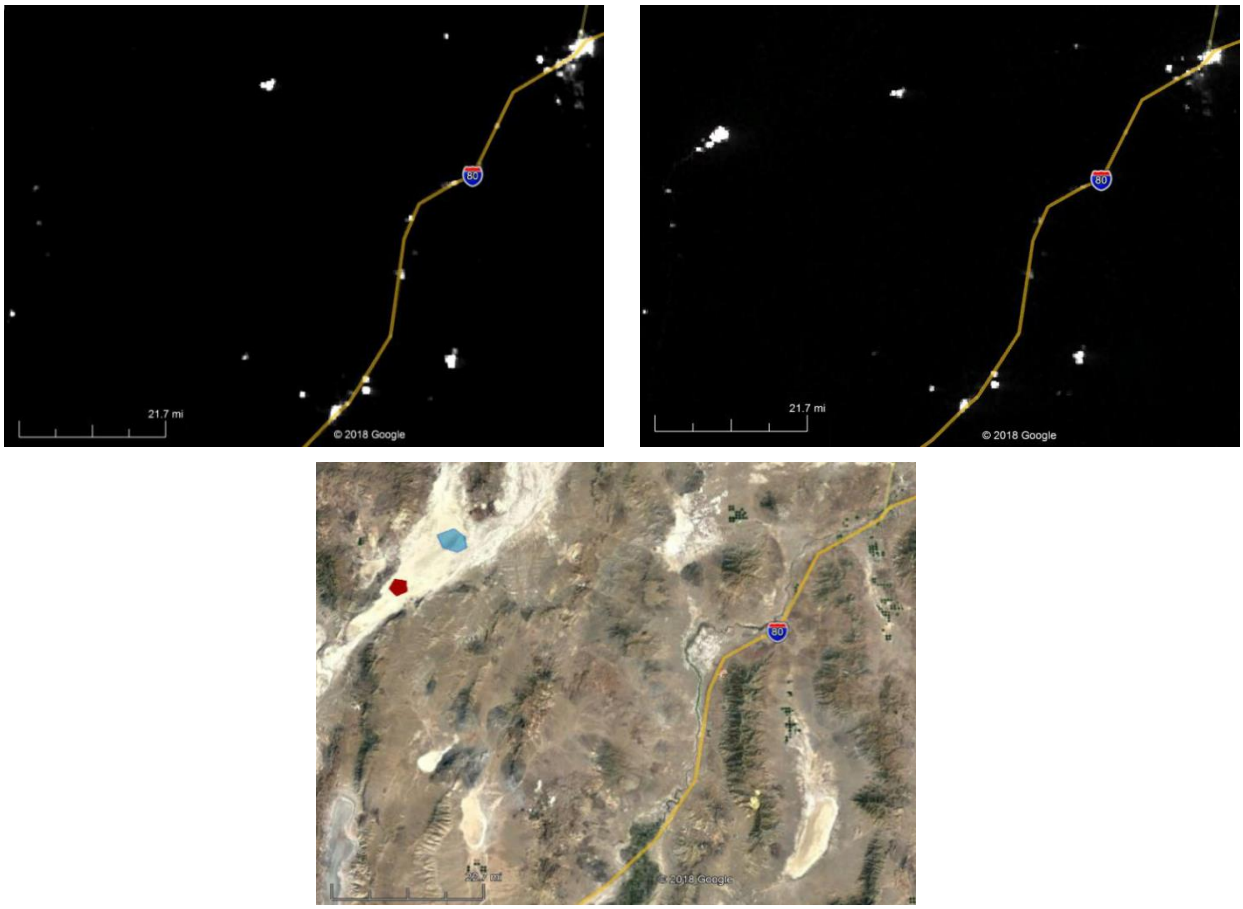

Figure 3.3. Example nighttime satellite imagery.
A) Nighttime satellite image of the Northern Nevada area during moonless, cloudless nights during the month of July, 2016. The bright spot in the upper middle portion of the image is Sulphur, Nevada and the Hycroft mine. The fainter spot near the left border almost half way down in Gerlach. The major feature on the upper-right is Winnemucca. B) is the same region in August 2016. The major feature on the left of the image is Black Rock City. C) Orientation map showing Black Rock City site (red pentagon), and the control playa site (blue area; Map data: Google, DigitalGlobe).

An example of one of the resulting GeoTIFF images can be seen in Figure 3.3B. Comparison of the image with the underlying geography, as seen in Google Earth (Map data: Google, DigitalGlobe), reveals that the Black Rock City area is quite clearly resolved from surrounding communities. The amount of light radiating from Black Rock City and other sites of interest in this sparse ALAN environment can, therefore, be measured by placement of an aperture around the area of interest and integrating the energy readings.

3.1.2 Monthly Composite Satellite Data

The Earth Observations Group (EOG) at NOAA/NGDC is producing a version 1 suite of average radiance composite images using nighttime data from the Visible Infrared Imaging Radiometer Suite (VIIRS) Day/Night Band (DNB). Prior to averaging, the DNB data are filtered to exclude data impacted by stray light, lightning, lunar illumination, and cloud-cover. Cloud-cover is determined using the VIIRS Cloud Mask product (VCM). In addition, data near the edges of the swath are not included in the composites. Temporal averaging is done on a monthly and annual basis [6].

The products are produced in 15 arc-second geographic grids and are made available in GeoTIFF format as a set of 6 tiles. Each tile is actually a set of images containing average radiance values and numbers of available observations.

In the monthly composites there are many areas of the globe where it is impossible to get good quality data coverage for that month. This can be due to cloud-cover, especially in the tropical regions, or due to solar illumination, as happens toward the poles in their respective summer months. Therefore, it is imperative that users of these data utilize the cloud-free observations file and not assume a value of zero in the average radiance image means that no lights were observed.

The Version 1 monthly series of composites is run globally using two different configurations. The first excludes any data impacted by stray light. The second includes these data if the radiance vales have undergone the stray-light correction procedure [6]. These two configurations are denoted in the filenames as "vcm" and "vcmsl" respectively. The "vcmsl" version, that includes the stray-light corrected data, will have more data coverage toward the poles, but will be of reduced quality.

The files are obtained as compressed tarballs, each containing a set of geotiffs. Files with extensions "avg_rade9" contain floating point radiance values with units in nanoWatts/cm^2/sr. Note that the original DNB radiance values have been multiplied by 1E9. This was done to alleviate issues some software packages were having with the very small numbers in the original units. Files with extension "cf_cvg" are integer counts of the number of cloud-free coverage, or observations that went into constructing the average radiance image. Files with extension “cvg” are integer counts of the number of coverages or total observations available (regardless of cloud-cover).

The data files to be used were segmented to a rectangular region encompassing Black Rock City and surrounding area in northern Nevada (coordinates: Upper Left (119d27'21.05"W, 41d29' 8.15"N); Lower Left (119d27'21.05"W, 39d38'25.94"N); Upper

Right (117d33'17.12"W, 41d29' 8.15"N); Lower Right (117d33'17.12"W, 39d38'25.94"N). The amount of light radiating from Black Rock City and other sites of interest was measured by placement of an aperture around the area of interest and integrating the energy readings.

The composite images provide a useful overall view of the magnitudes of ALAN but have several limitations. They are biased by averaging only the moonless, clear nights of a month which skews the data. In addition, they are not suitable for the analysis of zenith angle dependency of the radiance.

3.1.3 Population Census Data

Population estimates for Black Rock City and event dates (see Appendix D) were obtained from records maintained and provided by Black Rock City, LLC[1].

Population density for other Nevada communities was provided by the U.S. Census Bureau. The data were extracted from TIGER/Line® shapefiles for the 2010 census [7] which was the latest complete census. Total Black Rock City population used in the calculation of the Light at Night Index (LANI) included attendees, staff, volunteers and health and safety personnel for a total of 79,379 for 2017.

3.1.4 Statistical Analysis

Statistical and graphical analyses were performed primarily using Excel (Microsoft, Seattle WA). Testing for the difference between sample means was done using a two-sample *t*-test. Calculations were completed using the Solver function in Excel. Non-linear model optimization was accomplished using CurveExpert (Hyams Development, https://www.curveexpert.net/) which utilizes the Levenberg-Marquardt method to solve nonlinear regressions.

3.2 Ground Data

3.2.1 Ground Data Protocols

As specified in the Contract an effort was made to replicate a protocol for ground-based observations of event related LAN similar to that done in 2011 by the BLM. The protocol was developed by the National Park Service (NPS) and is summarized in a document they produced that is attached as Appendix B (the "2011 Protocol"). As documented in this report that protocol was substantially repeated for the 2017 event.

A severe constraint on the 2011 Protocol is the need to make observations between astronomical twilights and in the absence of moonlight. Because of the short duration of

[1] Benson, Marnee (Associate Director of Government Affairs Burning Man), personal communication.

the Burning Man event, and the happenstance of its timing, the only practical nights for collecting the ground-based data were 27-29 August 2017. We note that 27 August was the first formal night of the event and that the optimal usable window was shorter on each successive night due to phase progression of a waxing gibbous moon.

Per the 2011 Protocol, two nights were allocated for making observations. The most critical quantitative brightness measurements were assigned to the first night on the premise that if something were to go wrong it might be possible to recover on the following night. The second night was reserved for qualitative observations to be made in the event venue itself, a lower priority data set.

The other constraint, weather, was acceptable, but not ideal. The nights available were quite dark, but were affected by intermittent scattered cloud. Fortunately, the clouds were relatively few and discrete, exposing large tracts of clear sky between them. Nonetheless, not all of the qualitative observations were possible at each of the observing sites.

On 26 August WRC personnel travelled to the event site and spent the afternoon locating suitable observing sites and recording GPS coordinates for each. The goal was to mark about six locations in roughly 2-mi increments distance from the center of Black Rock City. In spite of earlier concerns about flooding on the Black Rock Playa, the playa was dry and devoid of plant-life, making it quite suitable for nighttime observations (Figure 3.4).

Figure 3.4. WRC personnel mark the GPS coordinates.
Marking coordinates of Site Number 1, 12-mi from Black Rock City on the distant southern horizon.

The observing sites chosen are tabulated in Table 3.1. Site number 0 is the Black Rock City center. The distance, d, to each observing site from site 0 is calculated in statute miles using the Haversine Formula commonly used in spherical astronomy and celestial navigation [8]. Locations of the observing sites are shown graphically in Figure 3.5.

Table 3.1. Ground observation locations.

Site No.	Latitude	Longitude	Distance[1] [mi]
0[2]	+40° 47.207	-119° 12.398	0.0
1	+40° 56.905	-119° 07.225	12.0
2	+40° 55.406	-119° 08.340	10.1
3	+40° 53.859	-119° 09.395	8.1
4	+40° 52.316	-119° 10.392	6.1
5	+40° 50.781	-119° 11.472	4.2
6	+40° 49.255	-119° 12.458	2.4

[1]distance, d, of each site from site 0, the Black Rock City center.

[2]coordinates for Black Rock City center from Google Maps.

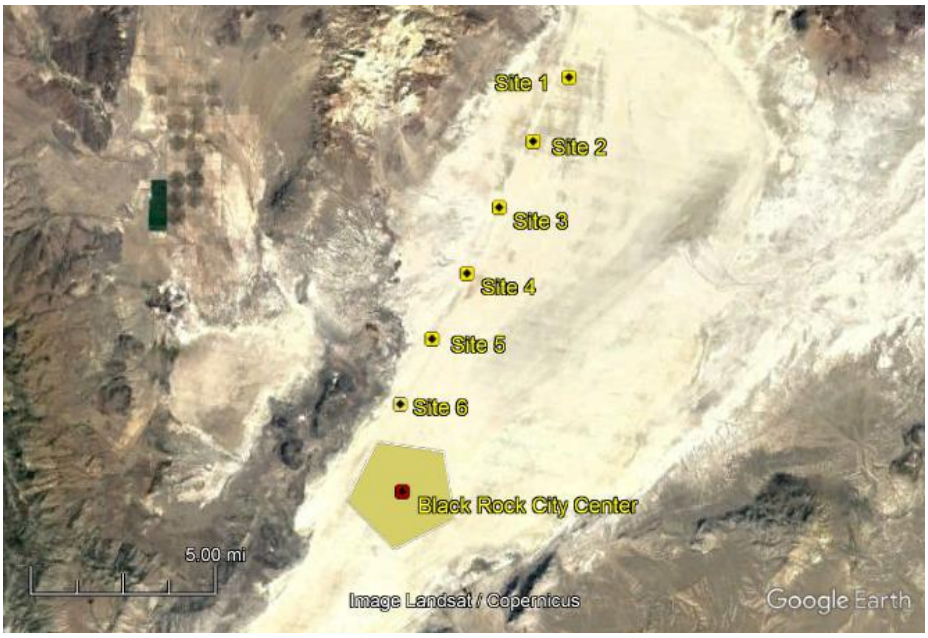

Figure 3.5. Ground observing sites shown on Google map.

On 27 August two WRC personnel returned to the event site. Because the time window for observations was short, and in the interest of most efficiently using that time, the team re-positioned at the most distant site (Site number 1, 12-mi to the NNE of the event) and worked progressively closer to the event as the night wore on. Following evening astronomical twilight and moonset the measurement protocol commenced. All observations in the protocol were made and recorded by both observers as weather conditions allowed. Each observation sequence, including travel time to the next site, required about 30-45 minutes, just enabling acquisition of data at all six sites before the arrival of early morning astronomical twilight.

Prior to travelling to the site, WRC personnel had made copies of the 2011 Protocol data sheets, and had reconstructed a set of Visual Contrast Targets. Originals of both of these documents can be found in the flash drive accompanying this report. The observing team was also equipped with a new factory-calibrated SQM-L photometer, and Canon 70D SLR and S95 cameras as specified in Appendix B.

Each observer made three sets of quantitative measurements at each location: 1) three measures at the zenith, 2) three measures at the horizon in the direction of Black Rock City (Source), and 3) three measures of a dark region of the horizon orthogonal to the direction to the Source (Dark Horizon). The remaining observations were all subjective psycho-visual observations: 1) appearance of ALAN in the nocturnal scene, 2) visual contrast, 3) limiting magnitude, and 4) appearance of Milky Way and zodiacal light.

On the evening of 28 August WRC personnel entered the event venue to make qualitative observations and photographs.

3.2.2. Ground Data Inventories

An inventory of the data collected from the ground-based survey, and archived on the flash drive accompanying this report (Appendix A), includes the following:

- GPS coordinates of each site.
- 12 2011 Protocol format data logs with qualitative (psycho-visual) observations, two for each of six sites.
- 36 sets of SQM-L measurements, six for each of six sites.
- X Canon 70D photographs, both JPG and RAW formats.
- Y Canon S95 photographs, both JPG and RAW formats.

4. Results

4.1 Satellite

4.1.1 Overview of regional/ temporal ALAN observations

As the 42nd most populous state, Nevada is sparsely populated with a density of 26 people per square mile [9]. Nevada is largely a desert and about 86% of the state's land is managed by various jurisdictions of the U.S. Federal government. It is not surprising then that much of Nevada has very little ALAN compared to other more populous regions of the country. Figure 4.1 is a nighttime satellite view of Nevada and is remarkable for vast areas of the state which provide an abundance of naturally lighted habitat.

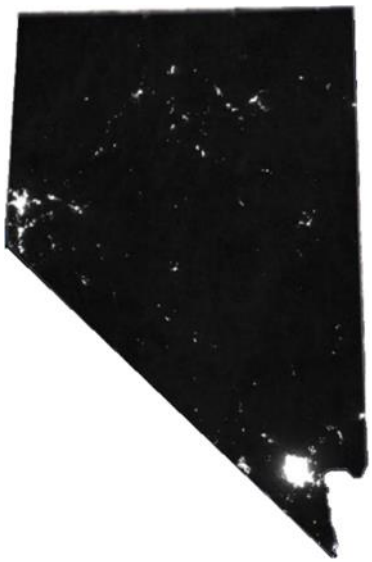

Figure 4.1. Nevada ALAN from oblique satellite view (August 2016).

The output of ALAN by a community is a dynamic property that varies by night and by time of year. The monthly average radiance for sites in northern Nevada is shown in Figure 4.2. The city of Winnemucca is a notable feature which varies month-to-month with an increase in radiance observed during the winter months of December through February. The Rochester open pit gold mine produces a smaller but more stable radiance throughout the year with a small increase during the winter. Black Rock City, however, is a unique community that only exists for a short period during the year. Most of the year there is essentially no ALAN and significant ALAN radiance is limited to a period in August with some spillover into September. The purpose of this report is to characterize the ALAN produced during this limited time period in greater detail and produce a record for quantitative comparison with future levels of ALAN.

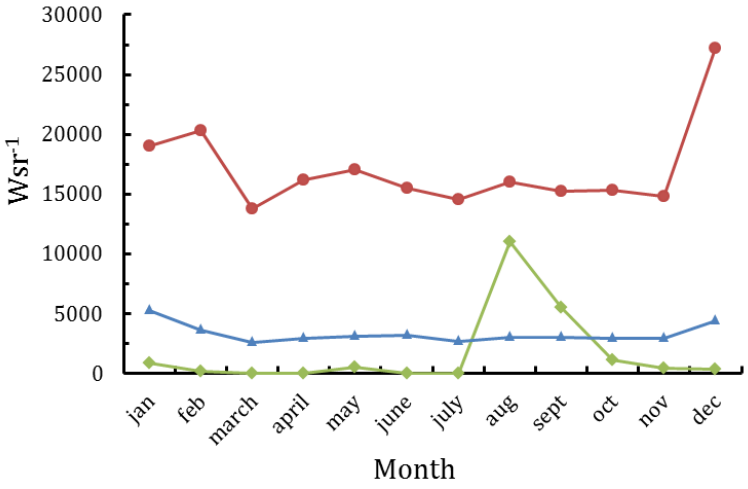

Figure 4.2. Monthly average radiances for three locations in Nevada.
The green line is radiance of Black Rock City, the red line is Winnemucca and the blue line is the Rochester mine.

4.1.2 ALAN zenith angle characterization

The amount of ALAN observed, as a function of satellite zenith viewing angle, is an interesting property that can be quantitatively related to the efficiency of community lighting. Light from shielded sources, or downward-directed light, that is scattered from the earth's surface has an intensity maximum at a zenith angle of 0° (i.e. straight up). Light that is directed upward, however, will have a maximum intensity where it is pointed. For example, light from car headlamps and many unshielded light sources have above-horizon maxima at high zenith angles, resulting in satellite observations of greater radiance at zenith angles 50-80° than near the zenith. Much of that light could be considered wasted lighting. Looking at the satellite observed radiance as a function of zenith angle is, therefore, instructive regarding the amount of wasted ALAN.

The zenith angle dependency of nighttime radiance associated with the Black Rock city and the Burning Man event was determined and is shown in Figure 4.3. The results are compared with Sedona, AZ and Tucson, Arizona. Sedona, AZ is a recognized Dark Sky Community [10] that has taken regulatory steps to minimize production of ALAN. Tucson is a large community that has a typical ALAN profile. Due to a limited number of observing nights and dynamic ground conditions, the data for Black Rock City have a greater variance than the comparison cities, but it is clear that Black Rock City has a significant increase in radiance at the higher zenith angles. This pattern is similar to that observed for Tucson, but a definite contrast to that of Sedona, which actually decreases at the higher zenith angles. This indicates significant amount of poor shielding and/or misdirected light above the horizon for Black Rock City.

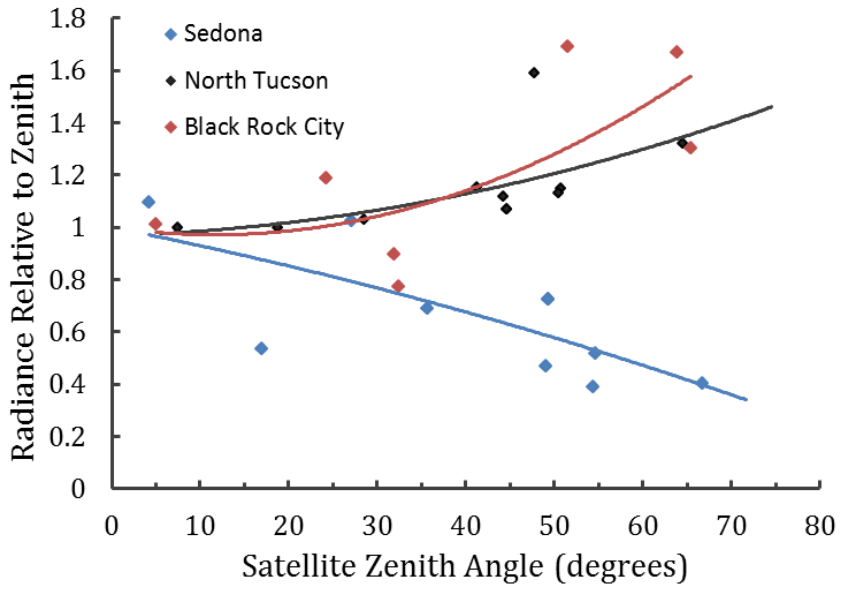

Figure 4.3. Example zenith angle (ZA) curves for three communities. The radiance observed (relative to that observed at a near 0° ZA) is plotted for a range of ZA values up to about 70°. The blue symbols are for Sedona, AZ (a certified Dark Sky Community), the black symbols are for North Tucson, AZ and the red symbols are for Black Rock City, NV (during the Burning Man event).

4.1.3 Temporal Measures of ALAN

The Burning Man event lasts for 8 days; however, the ALAN at the site is measurably increased for about 4 weeks before and a week after. The radiance at the site was monitored nightly during this period to provide a detailed timeline of the magnitudes of ALAN during the example period of 2016 (see Figure 4.4).

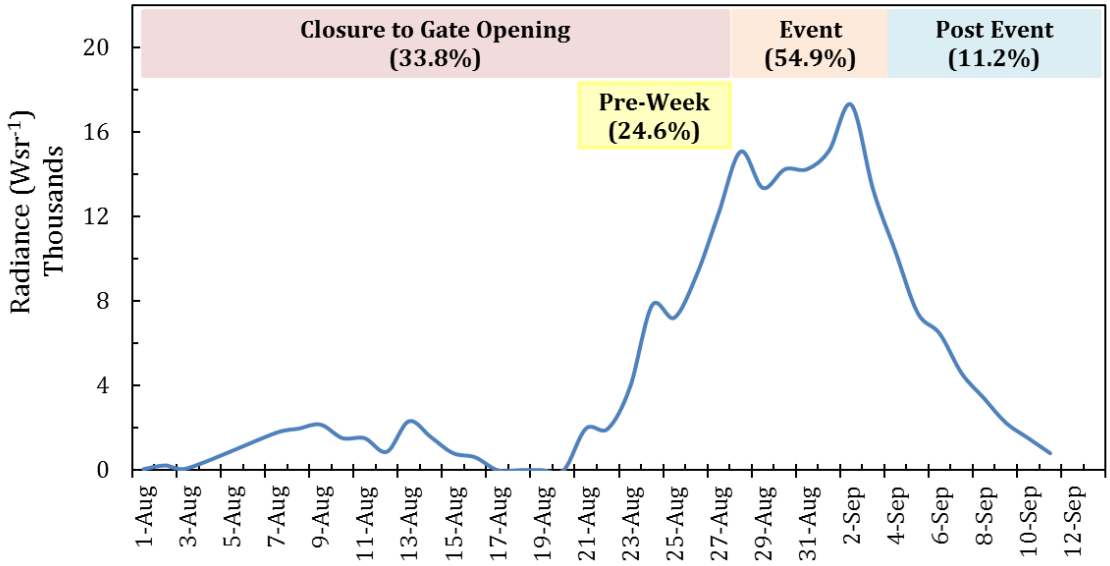

Figure 4.4. ALAN around the time of the Burning Man event (2016).
The percentage of total radiance over the Black Rock City site between site closure and opening of event gates, one week prior to gate opening, during the event and post event is indicated. Note that the dates are the time at which satellite imaging was performed which is offset from the calendar date of the event. For example, the event opened gates on Sunday August 28. The ALAN measurements for that night were obtained early in the morning of Monday August 29.

As expected, the nights with the most intense ALAN (> 12,000 Wsr^{-1}) occur within a few days prior to and during the actual event. Integration of the radiance over the site closure period (August 1 through September 21) revealed that about 54.9% of ALAN associated with the Burning Man event was observed during the event. Significant ALAN (>3500 Wsr^{-1}) was observed for six days before the event and 2 day after the event. About 24.6% of the total radiance associated with the Burning Man event was observed during the week prior to the event. After the close of the event the level of ALAN rapidly diminishes, with only about 11.2% of total radiance observed after the close of the event.

These detailed measurements show measurable levels of ALAN above natural background levels for about a 6 week period. However the measurements confirm that

ALAN associated with the Burning Man event is primarily concentrated in a narrow window of time, with 79.5% of the ALAN occurring during a 15 day period out of the year.

The average radiance per night during the Burning Man event from years 2012-2017 was also examined, and is presented in Figure 4.5. The data can be fit using a second degree polynomial with a high coefficient of determination (r^2 = 0.97). The data show a trend of increasing amounts of ALAN since 2014. The rate of increase in ALAN would appear to be increasing although the period of observation is short and the longer term trend would require acquisition of further data for a more accurate characterization.

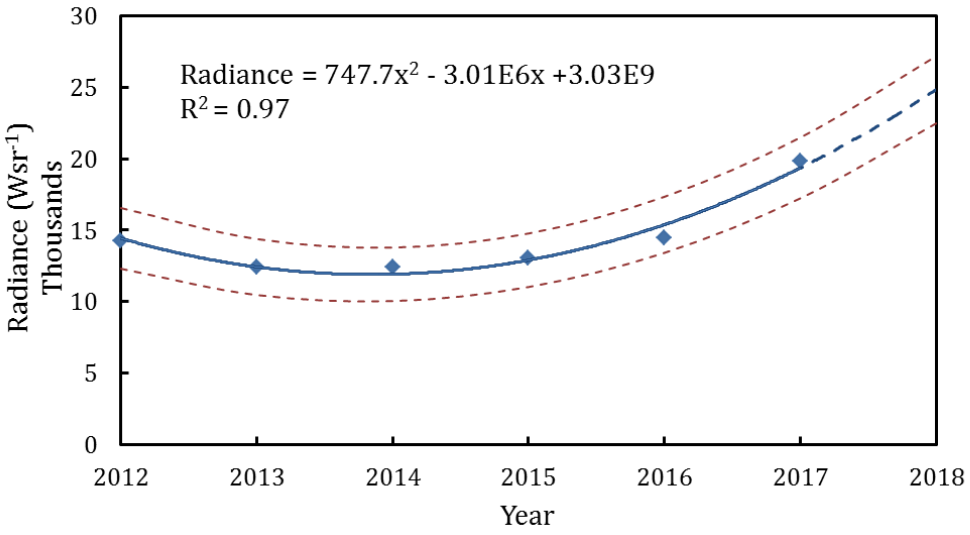

Figure 4.5. Average nightly radiance during event by year.
The blue diamonds are the average nightly radiance. The blue solid line is the best second degree polynomial fit to the data points. The dashed blue line is the extrapolation of the fit to future years. The dashed red lines indicate the 95% confidence predictive interval for the fit.

This model predicts an increase in ALAN in the absence of increasing population numbers, since the model is based upon relatively similar population profiles observed over the recent history of the event. If the current trend continues, this model would suggest an increase in ALAN of about 29% in 2018 over 2017. However, we note that polynomial models can easily over-fit data and are not very reliable for extrapolation. **Data from 2018-2020 would be particularly important in resolving the direction of the current trends.**

4.1.4 Impact of Population Totals on ALAN Radiance

The pioneering work of Garstang, published in 1986, documented the use of community populations as a surrogate for community radiance at night [11]. The population size at the event could then be anticipated to be an important determinant for observed radiance, and was, therefore, of interest to explore. The impact of population size was assessed using two methods. The first was to look at the radiance observed during the event as a function of an estimate of the population present the night of the observation.

The second was to examine the average radiance of the event as a function of the average population present during the event that year.

For the first approach the population present for the nights just before and during the event were compared to the radiance detected by satellite. The nightly radiance (corrected for moonlight and normalized for satellite zenith angle) was plotted against the population for nights during the 2012 through 2017 events, and is shown in Figure 4.6. There is a strong correlation (r = 0.94) of radiance with the population at Black Rock City. The data suggest a decreasing relative impact of increasing population after about 15-20 thousand. The initial steep rise in radiance observed with populations up to 10,000 occurs with the population present prior to opening of the gates (yellow symbols in Figure 4.6). These people are associated with installation of "infrastructure lighting" which is presumably largely completed by the time the gates open. The ALAN levels are approaching their maximum at that time with a more modest rate of increase as the population swells during the event. Therefore, increasing the population of attendees would be expected to have a relatively small impact on the average radiance per night.

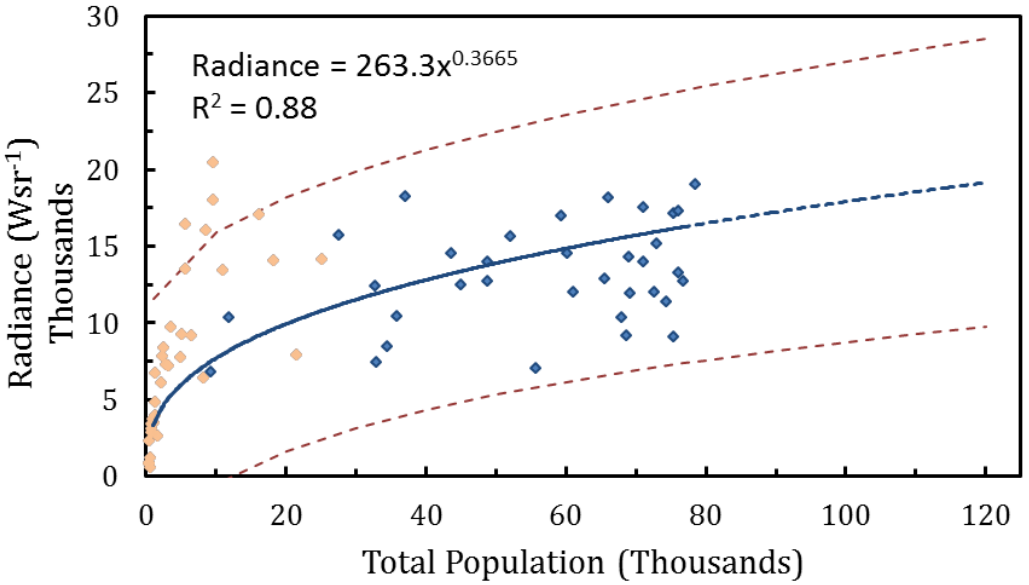

Figure 4.6. Correlation of ALAN with Burning Man population.
The total population present at the Burning Man event was provided by Black Rock City, LLC and correlated with the normalized radiance measured by satellite imaging. The yellow symbols are from nights prior to gate opening and the blue symbols are from nights during the event. The radiance was modeled as a power function of total population with a high coefficient of determination of 0.88 (or a correlation coefficient of 0.94).

The second approach is to look at the average nightly radiance for the event over the years 2012-2017, as the total attendance each year may differ. This analysis is shown

graphically in Figure 4.10 and shows the average radiance during the event to be independent of increasing total population. This result is consistent with the findings of Figure 4.6 considering that the population during the event is greater than the observed approximately 20,000 "saturation" level. The trend has been plotted as a linear function of average total population during the events for years 2012-2017. The number of points, however, is small resulting in greater uncertainty in the trends.

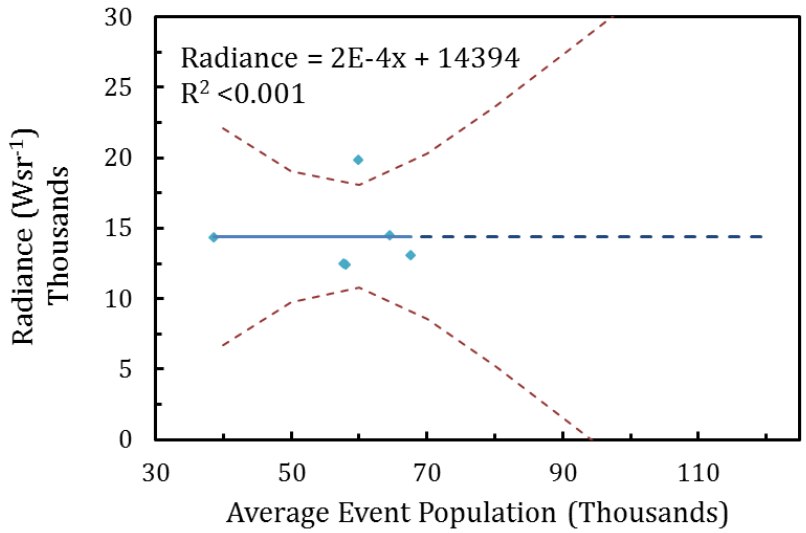

Figure 4.7. Average radiance per event population.
The blue symbols are the average event radiance. The solid blue line is a linear fit to the data while the dashed blue line is the predicted radiance. The red dashed lines are the 95% predictive interval for the data. The data points, left to right, are from year 2012, 2014, 2013, 2017, 2016, 2015.

The trend analysis of the change in ALAN radiance with population at the Burning Man event, shown in Figure 4.6 and 4.7, provides two models for the prediction of the change in ALAN that would occur if the population at Black Rock City were to be increased. The best statistical model is Model 1, which has the larger and more complete data set. For an increase in the average daily population during the event from current levels of about 70,000[2] to a total population of 90,000, Model 1 predicts an increase in ALAN of only 9.6%. Model 2 predicts an increase in ALAN of only 0.03% for an increase in total population to 90,000 (see Table 4.1). These are modest increases for an increase in population of 28.6%.

[2] 70,000 chosen based upon average nightly 2017 population of 65,000 with a peak of about 80,000.

Table 4.1. Prediction of impact of increased population upon ALAN.
Predictions based upon trend data from 2012-2017 and are relative to a baseline average total population of 70,000.

Total Population*		Increase in Nightly Average Radiance (%)			
Number	Increase (%)	Model 1†	95% UL	Model 2‡	95% UL
70,000	0	0.0	0.0	0.0	0.0
80,000	14.3	5.0	61.8	0.02	64.0
90,000	28.6	9.6	67.1	0.03	89.1
100,000	42.9	14.0	72.1	0.05	114.9
110,000	57.1	18.0	81.4	0.06	141.1

†Model 1, based on within event correlation of population and radiance.

‡Model 2, based on yearly event average radiance per average population.

The predicted change in ALAN with changing population is dependent upon a constant radiance per person and that there are no fundamental changes in the lighting characteristics of Black Rock City. However, examination of the radiance per person over recent years has shown this to be somewhat variable (see Figure 4.8). After relatively stable values of radiance per person from 2013-2016 a significantly increased value (approaching that observed in 2012) was measured in 2017. The increase in radiance per person tracks with the increased trend in average ALAN observed in 2017 (see Figure 4.5). It is unclear if these changes in ALAN observed for 2017 represent an increasing trend or if it is approaching a maximum value. If the radiance per person is trending higher the predicted impacts of population on ALAN presented in Table 4 would be underestimates. **Future measurements would be required to determine if new trends are being established both in total radiance and radiance per person.**

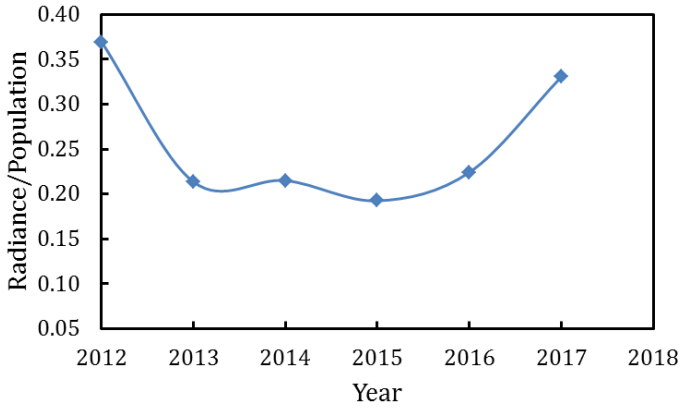

Figure 4.8. Change in radiance per person from 2012-2017.
The average radiance during the event is divided by the average population onsite during the event for the indicated year is plotted.

4.1.5 Comparison ALAN between Nevada Communities

ALAN is an intrinsic part of modern life: it performs an important safety role in our communities, and is a byproduct of our activities. There are a number of reasons to minimize ALAN levels and this should be a goal of all communities. However, there is not a specific ALAN radiance value that can be cited as the best value. It is therefore instructive to compare communities and determine how communities are doing relative to each other. This comparison can be done by determining a Light at Night Index (LANI) as a metric of the efficient use of ALAN by a community.

The LANI is based upon the nightly average radiance of a community per population and is scaled with respect to values observed for the US mainland and Hawaii. The formula for the LANI index is:

$$LANI = \frac{(C_{RP} - Min_{RP}) \times 100}{Max_{RP}},$$

where C_{RP} is the community radiance per population, Min_{RP} is the national minimum radiance per population, and Max_{RP} is the national maximum radiance per population. Since Black Rock City is a transient city the values of radiance and population were obtained as average values during the Burning Man Event.

Black Rock City was ranked with other Nevada communities with populations of 10,000 or greater. Figure 4.9 shows a 1-percentile ranking of Nevada communities(so a larger percentile reflects a smaller radiance per population and more efficient use of ALAN). Although Black Rock City (during Burning Man event) is the tenth largest city in Nevada with a peak population of 79,379 (including attendees, staff and volunteers [12]), it has the third best LANI in the state (rank of 90.1). Twenty of twenty-three communities with a population greater than 10,000 have a poorer LANI than Black Rock City.

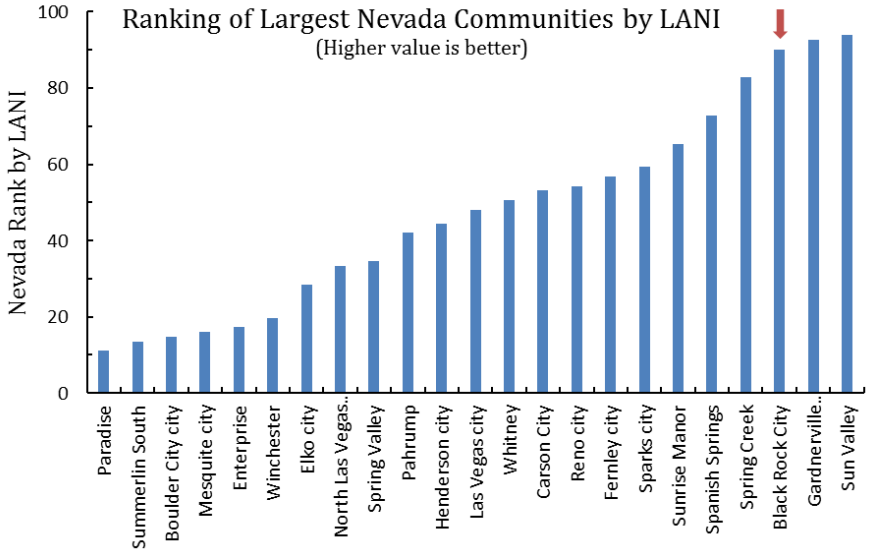

Figure 4.9. Percentile ranking of communities in Nevada.
Communities in Nevada, with populations greater than 10,000, are ranked by percentile with respect to LANI scores.

4.2 Ground Data

4.2.1. SQM-L Measurements

The SQM-L measurements from the raw data logs were migrated to a spreadsheet where the measurements for each site and each direction of observation were averaged and the standard deviation about the mean was computed. These summary values appear in Table 4.2. The site locations are indicated by the distance, d, from the Black Rock City center for each of the zenith, source, and dark horizon directions. Each brightness value is a mean of six measurements (three per observer). All measurements were made with a single instrument.

Table 4.2. Summary of SQM-L measurements.

Zenith			Source			Dark Horizon		
d [mi]	<brightness> [mag/arcsec^2]	std dev [mag/arcsec^2]	d [mi]	<brightness> [mag/arcsec^2]	std dev [mag/arcsec^2]	d [mi]	<brightness> [mag/arcsec^2]	std dev [mag/arcsec^2]
2.4	19.88	0.29	2.4	17.21	0.26	2.4	20.77	0.02
4.2	20.84	0.03	4.2	17.81	0.05	4.2	21.23	0.03
6.1	20.89	0.08	6.1	18.61	0.07	6.1	21.48	0.03
8.1	21.26	0.05	8.1	19.29	0.07	8.1	21.46	0.15
10.1	21.23	0.02	10.1	19.21	0.21	10.1	21.51	0.04

For each direction of measurement indicated in Table 4.2, a plot of the measured values as a function of d was made. These plots appear in Figures 4.10 through 4.12 respectively. The best line fit (logarithmic trend or shifted power) was applied to each of the data sets and the resultant equation appears in each graph.

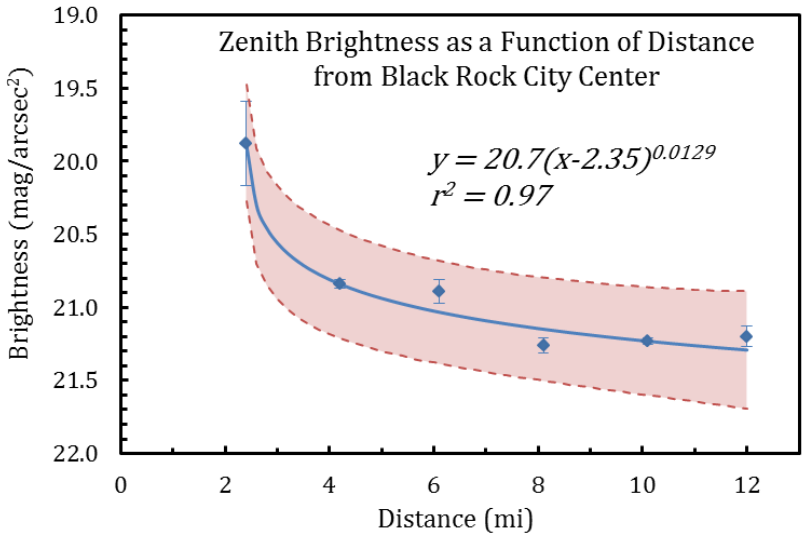

Figure 4.10. Zenith brightness.
The zenith brightness was measured as a function of distance from Black Rock City center. The equation of a shifted power trend line fit is shown. The standard deviation about the measurements is indicated by the blue limits and the shaded area indicates the 95% confidence interval about the fit.

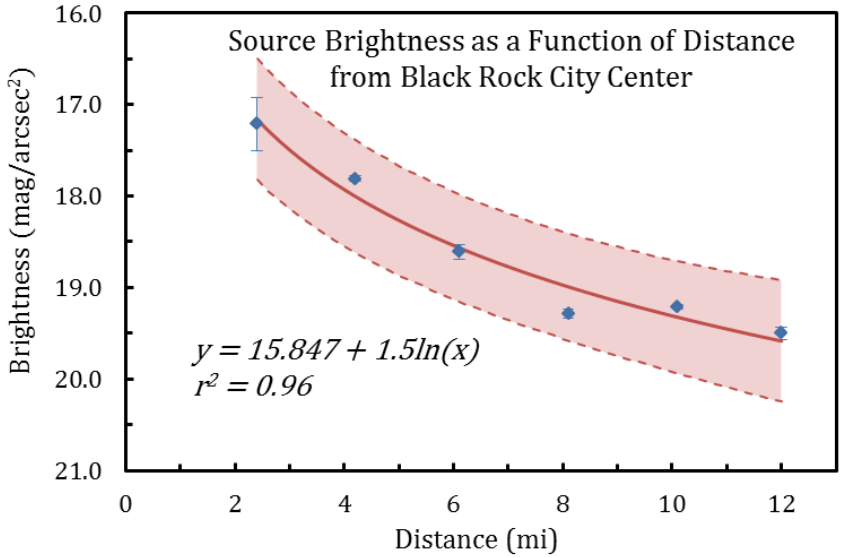

Figure 4.11. Source brightness.
The source brightness was measured as a function of distance from Black Rock City center. The equation of the logarithmic trend line fit is shown. The standard deviation about the measurements is indicated by the blue limits and the shaded area indicates the 95% confidence interval about the fit.

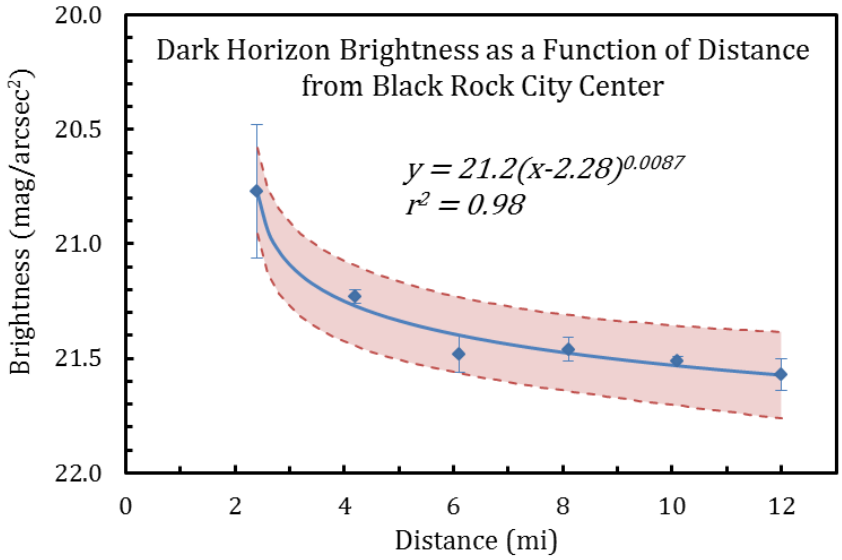

Figure 4.12. Dark horizon brightness.
The dark horizon brightness was measured as a function of distance from Black Rock City center. The equation of a shifted power trend line fit is shown. The standard deviation about the measurements is indicated by the blue limits and the shaded area indicates the 95% confidence interval about the fit.

4.2.2. Qualitative Observations

The qualitative observations were recorded on the raw datasheets used by the two field observers. The results were summarized on a single datasheet for each observation site; the summary sheets appear in Appendix F. The responses marked on the sheets are a "+" or "x" symbol, one for each observer. In some instances no viable response could be made, in which case the query was marked "n/a" for not applicable or not available. This was used specifically in the case of the text targets of varying font size on the Visual Contrast test, none of which were readable in dark conditions. It was also used in the event that cloud obscured specific stellar targets such that a limiting magnitude could not be determined during the time at a given observing site.

4.2.3. Photographic Observations

Photographs were made of the event site from each observing site and within the event venue. The photographs are stored on the flash drive accompanying this report. Some of the photography is in RAW format which provides higher dynamic range and the possibility of useful image processing and analysis. A detailed characterization of the Canon 70D quantitative photometry photographs is in the flash drive photography folder. Example images are shown in Figures 4.13 to 4.23 with captioned annotations.

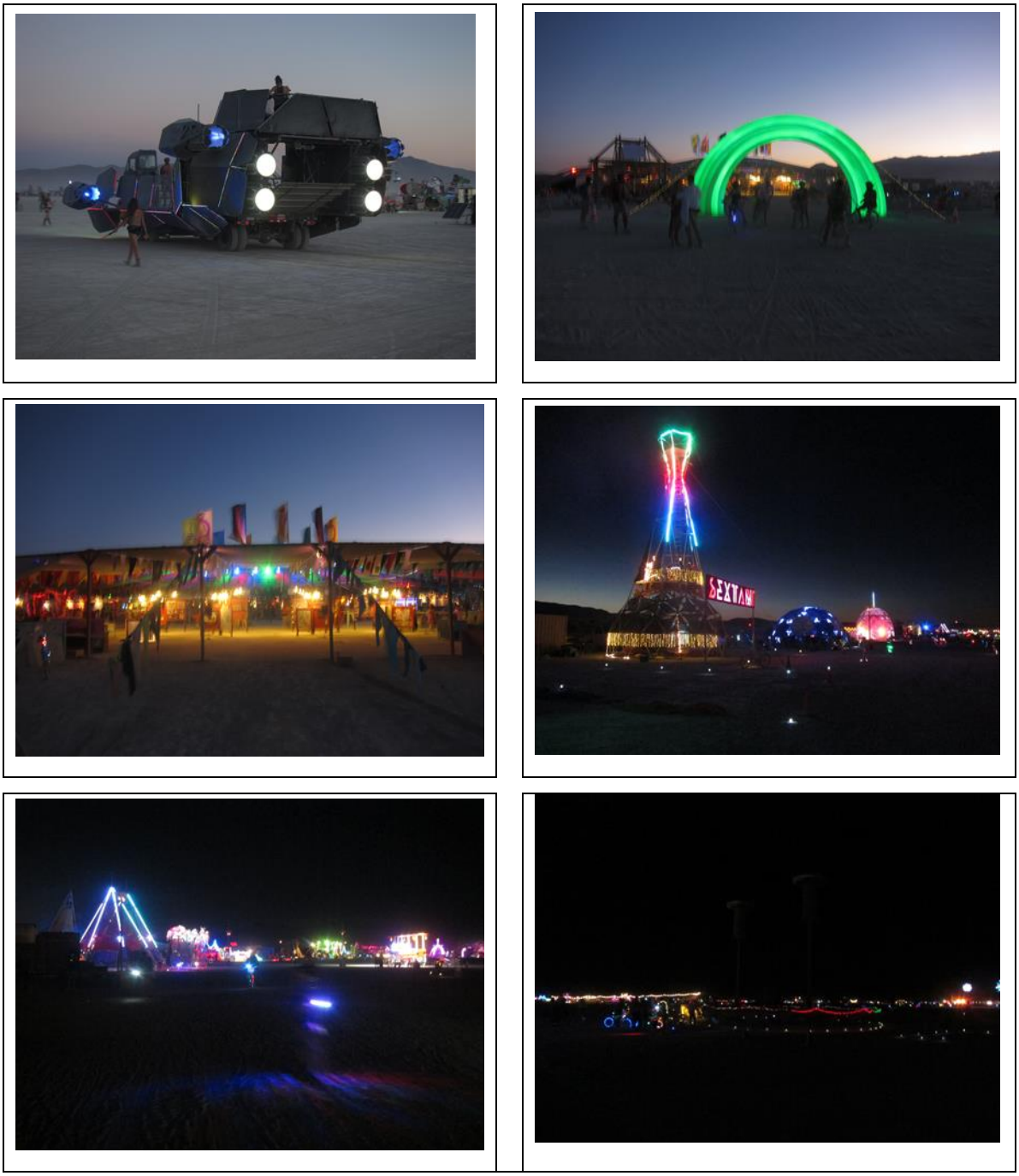

Figure 4.13. A photo montage of night time scenes.
Burning Man event venue, 8/28/2017.

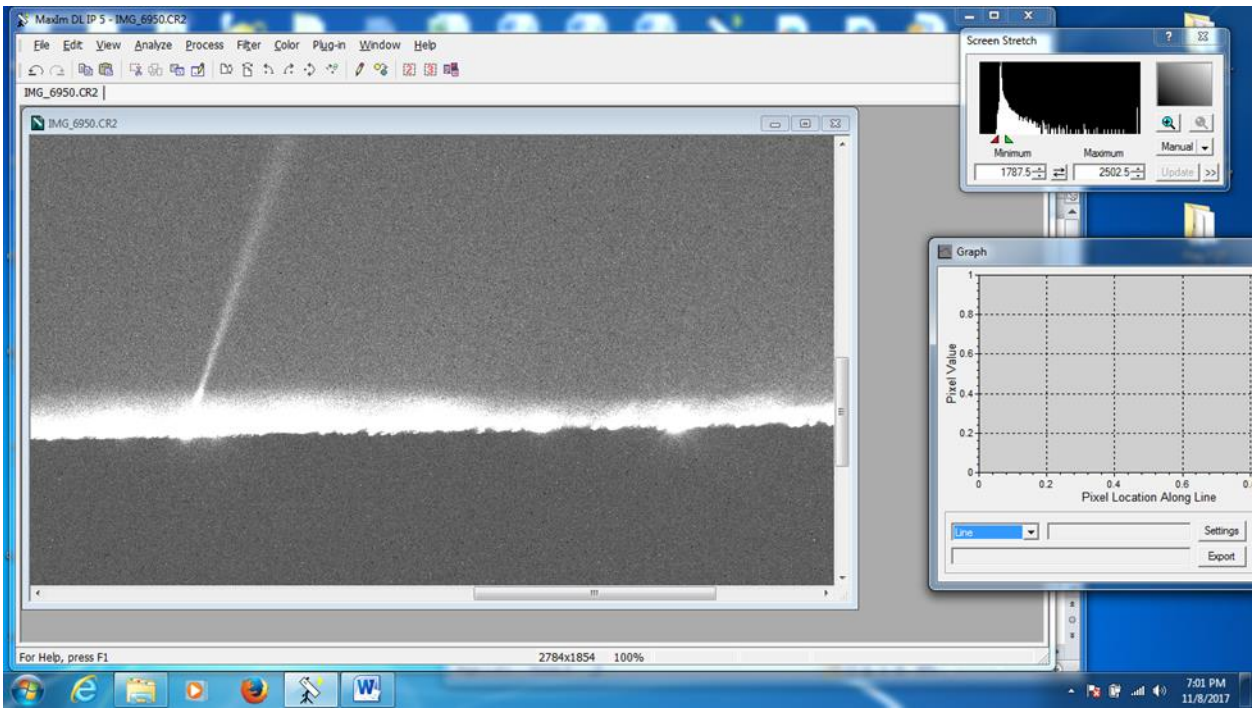

Figure 4.14. A RAW image of the Burning Man venue.
The image was converted to a monochrome image and displayed for digital processing on Maxim DL image analysis software. Of note is a bright laser beam directed skyward, 8/27/17.

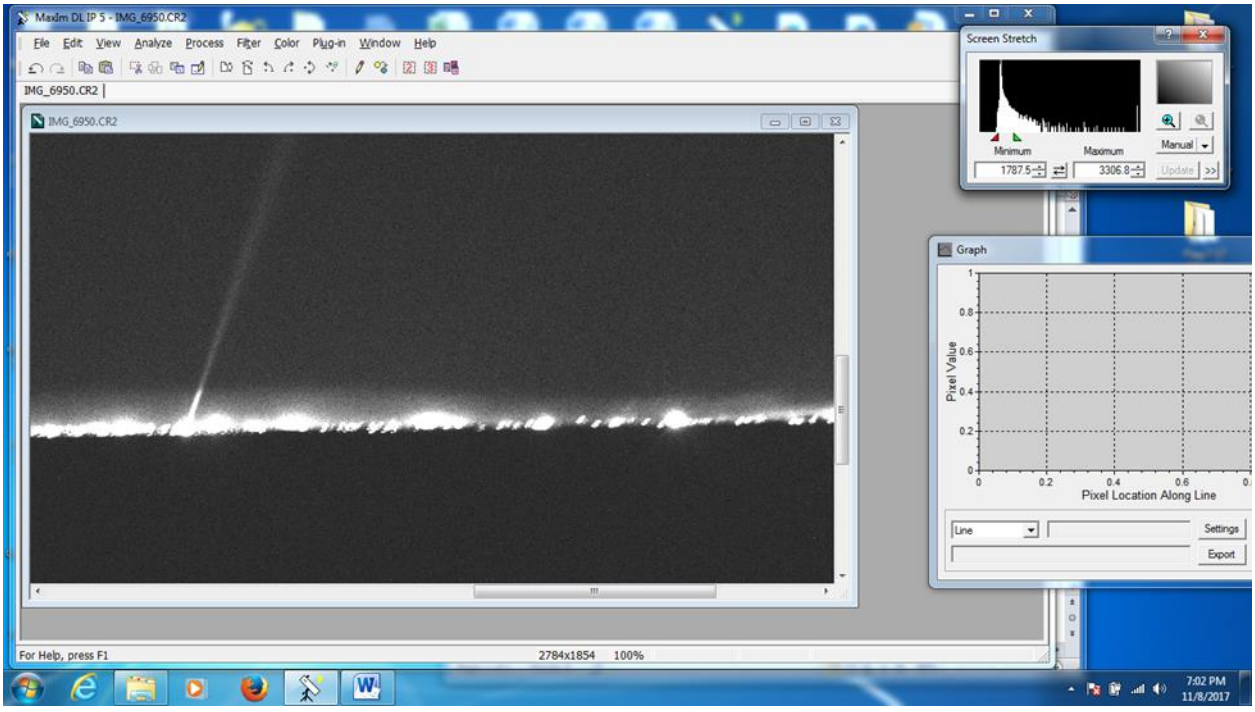

Figure 4.15. Image from Figure 4.14 with modified histogram, 8/27/17.
The modified image histogram provides more structure to the image. Note the very bright element of the laser beam which helps define the boundary of the dust layer.

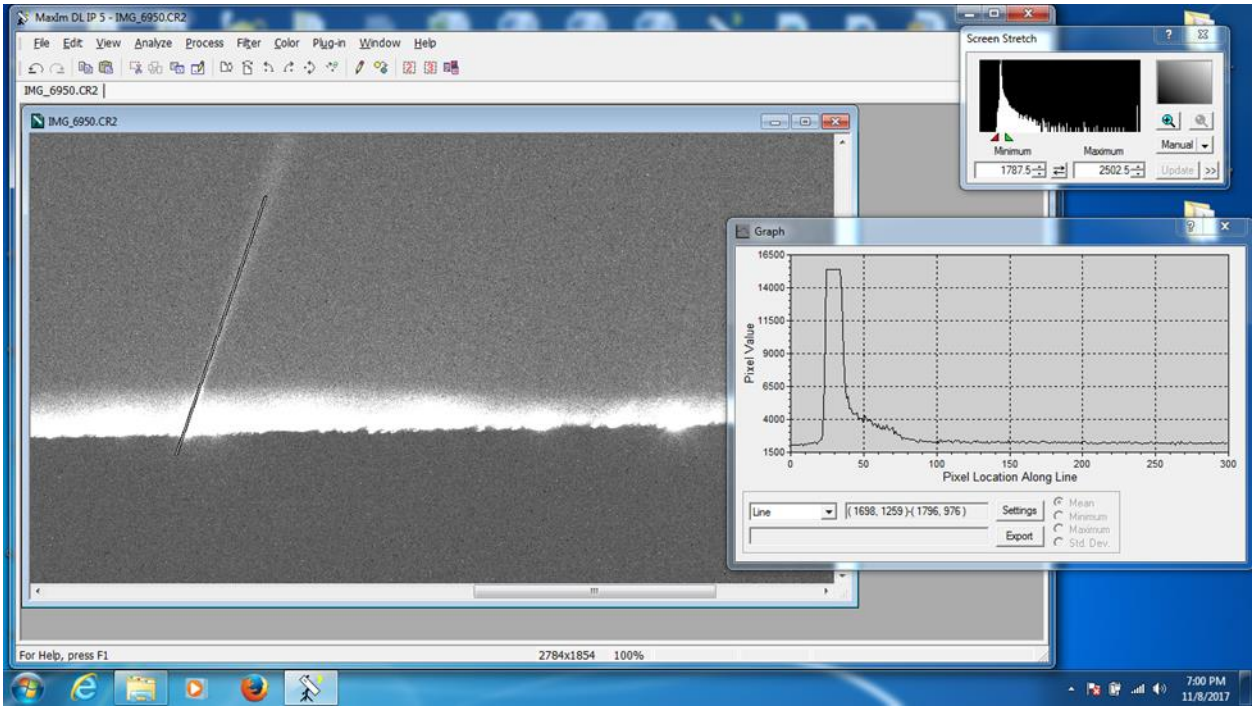

Figure 4.16. Line profile plotted along the length of the prominent laser beam. Image is the same as Figure 4.14, 8/27/17.

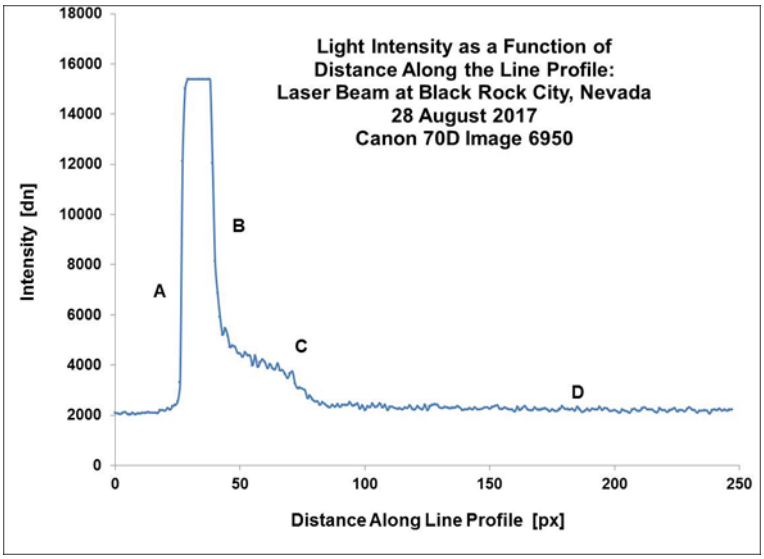

Figure 4.17. The line plot described in Figure 4.16.
The line plot starts at approximately ground level at left and extends to its termination in the sky above the event at the right of the plot. A represents ground level. The flat topped peak is the saturated light level of the bright part of the laser beam in the dust cloud overhead. B is a rapid decline in brightness of the laser beam as it transits the boundary of the dust layer. C is a gradual decline in brightness with some latent excess brightness due to residual dust particles lofted above the more discrete boundary. D is the steady decline of the laser brightness as it approaches sky background levels.

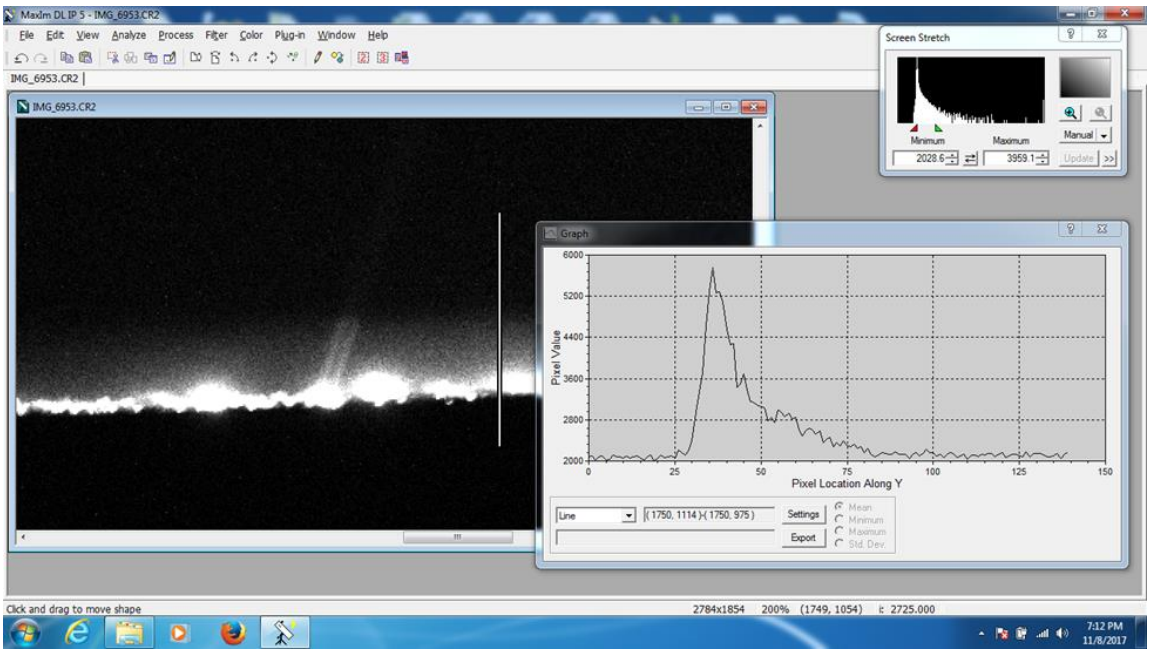

Figure 4.18. View of the Burning Man event (Canon 70D image 6953).
This image was made shortly after the image of Figures 4.14 through 4.16. In this instance we see two laser beams pointing skyward, but "terminating" sharply at the dust boundary layer. In this case there is a vertical line plot (see inset for the line plot graphic) which characterizes the scattering properties of the dust layer above the event, 8/27/17.

Figure 4.19. Dynamic Burning Man scenes.
The same scene photographed minutes apart suggests dynamic changes in the underlying spectral energy distribution attributable to rapidly cycling of colors of ambient lights. (Canon S95 images 1839 and 1840, 8/28/17)

Figure 4.20. View of Black Rock City from a distance of 4.1-mi (site 5).
The image is deliberately trailed to provide a distinct impression of the colors of the light emitted from the myriad sources of light at the venue. Contrary to first Impressions, this is not a spectrum. The horizontal axis is spatial, not spectral, dispersion. However, this does provide a good impression of the extreme and prolific range of colors to be seen and suggests that true spectroscopic observation would be very useful in future monitoring endeavors (see discussion in Section 5), 8/27/17.

Figure 4.21. Mast mounted portable work light.

The light was located at the 12-mi Road Entrance to Black Rock City. Typical of numerous such lights in the entrance, parking, and security areas on the south border of Black Rock City, 8/28/18.

Figure 4.22. Panoramic view of the Burning Man Event environment.
There are arrays of work/security lights on the center and right; the Burning Man site on the left. View from the southwest to the northeast. This image was made from Highway 34 south of the 12 mile Road junction, estimated on order of 1 mile from BRC center. (Canon S95 img1959, 8/27/18)

Figure 4.23. A close-up view of the mast mounted work lights.

The prominent light domes that they create are demonstrated. Most of this is wasted light, directed well above the horizon that does not contribute to the artistic efforts of the event and can be legitimately characterized as light pollution. These lights can adequately provide current levels of worker safety even if mitigated by shielding that reduces or eliminates the above horizon pollution. (Canon S95 img1976, 8/27/18)

5. Discussion

5.1 Evaluation of ALAN levels at Black Rock City

Quantitative measurements of ALAN produced in association with the Burning Man event at Black Rock City have confirmed that significant levels are limited to a short period of about six weeks. About 79.5% of that light is limited to about a 15 day period (e.g. see Figure 4.4). The Burning Man event is true to one of their main principles of "leave no trace" with respect to artificial light (which could be considered as a pollutant).

The average nightly radiance has been remarkably stable over the recent past from 2012 to 2016, despite a steady increase in the event average nightly population. However, this pattern was noticeably changed in 2017 with a significant increase in average nightly radiance (e.g. see Figure 4.5). In addition, the radiance per person increased in 2017. These increases are consistent with the model presented in Figure 4.5 and would predict further increases in ALAN in future years.

The brightening of Burning Man suggests some fundamental change in the event production which may be important to identify. This could be the result of increasing availability of power sources at the festival (e.g. number of reported generators and increased use of solar power have been reported[13]). Alternatively, there may be a change in the type of lighting employed (e.g. an increase in non-shielded sources associated with event activities and safety measures) or increased use of alternative festival specific lighting (e.g. search lights).

The model is based on a small number of years, however, and could represent a step-up to a new level or could be a transient elevation that will return to prior levels in the future. The resolution of this question will require future measurements to determine if the 2017 results are transient or if they represent a new or evolving trend in ALAN levels.

A possible future change to the Burning Man event could be an increase in the total population of people involved. Since the amount of ALAN is correlated with the total population (see Figure 4.6), an increase in population would be expected to have an impact on the amount of ALAN produced at the site. Table 4.1 presents the predicted impacts of increasing the population of people at Black Rock City for the Burning Man event. Based upon the trend observed from 2012-2017 and the within-year effect of population on levels of ALAN, an increase of the Black Rock City total population to 90,000 would be expected to have a relatively small impact on ALAN levels. The increase to 90,000 people (an increase of about 28.6% from 2017 levels) would be anticipated to increase the average nightly radiance by about 0.02-9.6%. These levels would still leave Black Rock City as one of the most "light efficient" communities in the State of Nevada as measured by the LANI.

However, if the 2017 measurements portend a new trend in ALAN levels a significant increase in ALAN, even in the absence of an increased population, can be expected (see Figure 4.7). Increasing the population would exacerbate this trend and it would be expected that the Black Rock City ranking among Nevada communities would

begin to deteriorate. **Follow-up measurements of 2018-2020 events are particularly critical to understanding the magnitude of the environmental impact.**

The zenith angle measurement of ALAN from Black Rock City was limited by conditions and the short sampling times available (about eight nights). The best data were obtained for the year of 2016 and these data indicated a significant increase in ALAN levels at higher zenith angles (see Figure 4.3). This finding indicates that a significant amount of the night lighting is not well shielded or is directed upwards. This lighting may represent wasted energy and could be categorized as light pollution. This data suggests that a significant amount of the ALAN could be mitigated through better shielding and light positioning.

5.2 Implications of the Ground Based Data

As noted in the original proposal discussions for this research, the protocol described in Appendix B is seriously deficient in scientific rigor (both quantitatively and qualitatively) and, as such, is generally of limited utility (see a separate discussion in Appendix C). In particular, comparisons between the original (2011) measurements and those reported here must be viewed with great caution. It is for this reason that the Contract specifically exempts extensive attempts to analyze these data.

Note, however, that the event photography suggested by the protocol does draw attention to two factors that could be productively explored in future event LAN monitoring: 1) the dust layer boundary above the event site has a profound effect on the perceived brightness of the event lighting, and 2) there is a broad range of colors represented in the event lighting that suggests analysis of spectral energy distribution (SED), as it could impact the environment, would be of considerable interest.

In spite of the carnival-like lighting and atmosphere of the event, on-site nighttime observers were impressed at how dark the venue generally appeared. Individuals walking through the event without a flashlight (or brighter and more colorful LED light strings) were virtually invisible except at very close proximity. Pedestrian lighting at night was really essential as a protective measure given the prolific and chaotic bicycle traffic (c.f. Figure 4.15).

This “dark community” impression, in spite of a population of about 80,000 people, is not a complete surprise given the temporary nature of Black Rock City with its total absence of a commercial support component. That is, no stores, shopping centers, car dealerships, schools, sports fields, etc. This is certainly one of the reasons that the LANI of the satellite data place Black Rock City so favorably with respect to permanent communities of similar population (see Figure 4.11).

5.3 Some Thoughts on Lighting Mitigation

Burning Man is a unique, short-lived event and, as such, is rather different in its impact and handling than would be permanent lighting in an established, on-going community; thus mitigation is a rather different issue than it might normally be.

It is apparent that much of the event-associated lighting is of "poor" quality from a normal "light pollution" evaluation perspective. This can be seen primarily in the zenith angle data and event photographs which characterize significant amounts of light as shining above the horizon. In terms of productive illumination for work or safety applications, this is wasted light that is known to have potential deleterious effects.

While we can characterize the quantity and character of the light, the extent to which it presents an undesirable environmental impact is subject to numerous considerations, and is ultimately the determination of the cognizant governing body.

The event is of short term and much of the otherwise poor quality lighting is integral to many of the art exhibits which are a major element of the event. On this basis it could be argued that at least some of such lighting may be best left alone. Likewise, high zenith angle lighting measured at the event is of a type that would be strenuously resisted by astronomical communities that are impacted by elevated sky brightness backgrounds. However, the short duration of the event, and the remote location of the site, have ensured minimal concerns from this sector.

Nonetheless, to the extent that there are environmental concerns, there are some specific areas that could be readily addressed:

- The event is often characterized by large, dense dust clouds; these aerosols contribute to significant horizontal scattering of light (especially blue light) that could have undesirable environmental effects. Thus, pro-active dust suppression at the event site could be beneficial.
- Extensive use of mast-mounted work lights peripheral to the event venue, but part of the support activities site, is problematical from three standpoints: 1) intrinsic high intensity, 2) extremely poor shielding, and 3) significant blue contribution to SED. These lights could be productively improved to provide a significantly better light environment through simple shielding interventions.
- The WRC team on-site observed the use of green lasers. Green lasers are generally higher energy, they can be deleterious to human vision, and they are a real potential threat to aircraft operations, even at considerable distances. The use of high energy green lasers should at least be discouraged if not stringently banned.
- Satellite data discussed in this report suggest that there may be changes taking place in the nature and/or quantity of light being generated during the event. This evolution may be independent, or loosely dependent, upon the attendance at the event. If this is true, then future efforts at mitigation could require registration of light sources and regulation of allowed lighting. This could be based on measureable factors such as light intensity, spectral energy distribution, and directional distribution of light energy.

5.4 Summary Conclusions

Broad conclusions of this study include:

- Although the ALAN levels associated with the Burning Man Event are in stark contrast to the natural levels present for most of the year, the ALAN levels are quite reasonable compared to other population centers in Nevada.
- Nonetheless, ALAN pollution levels may be impacted to a great extent by increased use of non-shielded lights and misdirected light sources (resulting in the increased radiance per person).
- Increasing the population at Black Rock City can be expected to have a small impact upon the level of ALAN.
- The average nightly radiance and the average radiance per person have increased, but the predictive model presented suffers from only a few years input. In addition the ALAN environment is dynamic and evolving. An accurate understanding of the trend in ALAN levels and the development of predictive models will require additional years of data to be added to the baseline established with this report.
- The 2011 Protocol is of limited utility and can be significantly improved. It should be replaced for future environmental impact monitoring.
- In spite of the special nature of the Burning Man event, there are LAN mitigation strategies that could improve the environmental impact of the event lighting.
- LAN measurement protocols have improved significantly since the 2011 measurements and at least some of those new protocols should be implemented in a coordinated, complementary way for future evaluation of the environmental impact of the event.

5.5 Recommendations for Future Event LAN Monitoring

We recommend that in order to understand the evolving LAN environmental impact of the Burning Man event the following steps be taken:

1. The satellite data presented in this report should be taken as an established baseline against which to compare future satellite measurements.
2. The satellite data protocol from this report should be repeated for multiple future Burning Man events, starting with the 2018 event.
3. The 2011 Protocol should be replaced by a new ground-based protocol commencing with the 2018 Burning Man event.
4. The new ground-based protocol would include:
    - On-site photography to document the nature and types of lighting used.
    - On-site spectroscopy to establish SED, and in particular fractional blue components of total radiance to augment satellite data.

- Small Unmanned Aerial Vehicle (sUAV) high dynamic range imaging (HDRI) to characterize the high zenith angle function of the event lighting.
- Twelve mile long radial transect continuous zenith recording of sky brightness during multiple nights of the event, and for different times of night. This would provide high temporal and spatial resolution measurements of variations in sky brightness attributable to the event itself.

6. References

1. Burning Man 2017 Special Recreation Permit Stipulations. (2017). Available at: https://eplanning.blm.gov//epl-front-office/projects/nepa/85572/115029/140474/20170729_SRP_BRC_2017_Stips_Signed_Decision_Letter_Attachment.pdf. (Accessed: 25th October 2017)
2. Irwin, A. The dark side of light: how artificial lighting is harming the natural world. *Nature* (2018). doi:10.1038/d41586-018-00665-7
3. NPP Mission Overview | NASA. Available at: https://www.nasa.gov/mission_pages/NPP/mission_overview/index.html. (Accessed: 30th November 2017)
4. Godin, R. Joint Polar Satellite System (JPSS) VIIRS cloud mask (VCM) algorithm theoretical basis document (ATBD). Joint Polar Satellite System (JPSS) Ground Project, Code 474, Doc. 474-00033. (2014).
5. NOAA's Comprehensive Large Array-data Stewardship System. Available at: https://www.class.ncdc.noaa.gov/saa/products/welcome. (Accessed: 16th November 2017)
6. Mills, S., Weiss, S. & Liang, C. VIIRS day/night band (DNB) stray light characterization and correction. in *Earth Observing Systems XVIII* **8866,** 88661P (International Society for Optics and Photonics, 2013).
7. TIGER/Line® with Data. Available at: https://www.census.gov/geo/maps-data/data/tiger-data.html. (Accessed: 15th November 2017)
8. Smart, W. M. Spherical Astronomy. *Camb. Univ. Press Lond.* 18 (1962).
9. Branch, G. State Area Measurements and Internal Point Coordinates. Available at: https://www.census.gov/geo/reference/state-area.html. (Accessed: 15th November 2017)
10. Sedona, Arizona (U.S.). Available at: http://www.darksky.org/idsp/communities/sedona/. (Accessed: 15th November 2017)
11. Garstang, R. H. Model for Artificial Night-Sky Illumination. *Publ. Astron. Soc. Pac.* **98,** 364 (1986).
12. Myrow, R. Burning Man Asks Nevada Officials for Permission to Grow to 100,000 | Art Wire | KQED Arts. Available at: https://ww2.kqed.org/arts/2017/12/08/burning-man-asks-nevada-officials-for-permission-to-grow-to-100000/. (Accessed: 18th January 2018)
13. DeVaul, D., Beaulieu-Prevost, D. & Heller, S. BRC Census 2016 Population Analysis.pdf. *Google Docs* Available at: https://drive.google.com/file/d/0BxJfvV_7__jqRTlpVHRWbGZIMkE/view?usp=sharing&usp=embed_facebook. (Accessed: 15th November 2017)

7. Appendices

A. Flash drive content.

This document provides a summary of the Contents of the Final Report Flash Drive which contains all of the final deliverables for EMPSi contract C-6077/001.

1. Final Report

This folder contains the Final Report document with all of its Appendices. The Final Report is a .pdf format file.

2. Ground-Based Data

This folder contains the ground-based raw data as follows:

- Completed log sheets
- Contrast target file
- Photo log
- Photographs

3. Satellite Data

This folder contains the satellite data as follows:

- 2012
  - Gtifs 16bit folder (nightly images of regions of interest)
  - Satellite data files
- 2013
  - Gtifs 16bit folder (nightly images of regions of interest)
  - Satellite data files
- 2014
  - Gtifs 16bit folder (nightly images of regions of interest)
  - Satellite data files
- 2015
  - Gtifs 16bit folder (nightly images of regions of interest)
  - Satellite data files
- 2016
  - Gtifs 16bit folder (nightly images of regions of interest)
  - Satellite data files
- 2016 Controls
  - Gtifs 16bit folder (nightly images of regions of interest)
  - Satellite data files
- 2017
  - Gtifs 16bit folder (nightly images of regions of interest)
  - Satellite data files
- Composites

- Spreadsheet 2012-2017
  - 2012_master_results.xlsx
  - 2013_master_results.xlsx
  - 2014_master_results.xlsx
  - 2015_master_results.xlsx
  - 2016_master_results.xlsx
  - control_results.xlsx
  - 2016_composite_results.xlsx
  - 2017_master_results.xlsx
- Control areas shapefiles
  - brc_playa_moonlight_control_area.dbf
  - brc_playa_moonlight_control_area.prj
  - brc_playa_moonlight_control_area.qpj
  - brc_playa_moonlight_control_area.shp
  - brc_playa_moonlight_control_area.shx

The above data files are provided for purposes of completeness of the report; it is not expected that these data will be needed by the client to use the Final Report. In the event the client wishes to explore these raw or processed data further, the originator of this Final Report will be available to interpret data should that be necessary.

B. 2011 protocol.

EXPANDED FIELD PROCEDURES FOR NIGHT SKY ILLUMINANCE

Experimental methods by National Park Service Night Skies Team, *8/21/2011*

Prior to Fieldwork

- Develop a simple datasheet, that includes location description, lat/long .
- Equipment - SQM-L marked with serial number, a micro fiber cleaning cloth, a dim red flashlight (to preserve night vision while writing), camera and tripod (the taller the better), GPS, star chart / planisphere, warm clothes, and safety equipment.
- Plan on 2-3 hours to conduct a transect containing 4-6 measures. Start the transect and observation after Astronomical Twilight and after moonset and complete the transect before moonrise. (http: //aa.usno.navy.mil/dataidocsIRS_OneYear.php).
- A digital SLR camera for documenting the view toward the event, at both wide angle (~50 mm) and telephoto (~300 mm). Ideally the camera atop the tripod is at the same height and position as the SQM-L measurements are taken from. Note that focusing at night usually requires manual lens and fast ISO.
- It is suggested to take a close-up photographic survey of lights at the event by walking through at night and capturing a sample of the kinds of lights that are being used. Also, any additional notes would be useful, such as "approximately 100 Colman lanterns, 40 temporary shop lights, etc."
- Record the GPS location for the approximate center of the event. This will enable field teams to get distances and aid with transect spacing. All distances should reference this center location.
- Familiarize yourself with the night sky at the time and date of fieldwork. A planisphere or free software like Stellarium will be useful for this.

Fieldwork Goal

- By taking a two transects, one along the flat playa and one along one of the valley sides, we can determine at what distance we would reach a threshold of 0.1 millilux illumination. We need not actually reach this threshold on a transect as it can be extrapolated with at least three sets of measures at different distances. This 0.1 millilux value is the environmental threshold used by the NPS for dark environments, and corresponds to the brightness of Venus just after astronomical twilight.
- Qualitative observations will be paired with the measurements to better understand what kind of visual impediment the artificial light is causing and to better correlate numerical data with a human experience. Photographic observations will aid these observations.

- A few examples of the astronomical magnitude system: Sun (- 27), Full Moon (- 14), Thin Crescent Moon (- 6), Venus (- 4), Sirius (- 2), Stars in Big Dipper (2), Dimmest star visible in a dark sky (7). Lower numbers are brighter on this logarithmic scale.
- The Sky Quality Meter-L units measure in astronomical magnitudes per square arc second. This is a luminance measure (not illuminance measure) and is expressed as brightness divided by area. Natural conditions at zenith is approximately 21.80. These can be converted to illuminance (total flux from a source) and is accurate at extremely low light levels and have a high dynamic range.

Qualitative Data Methods

These observations should be coupled with each quantitative measure. Each observer should have his/her own qualitative data and notes.

- Once photographs and quantitative measures are taken, make observations on the overall nighttime appearance and shadows on the data form. This is the top row in the data form. This includes overall appearance of the artificial light and how this "feels" to the observer, terrain illumination (under strong artificial light, ground texture can be easily seen, while under natural dark skies, only forms can be seen), the estimated extent of a light dome into the sky (use your fist at arms length to estimate 10° increments), and finally assess your own shadow as cast by any artificial light. Moving back and forth can help you detect your shadow.
- Using the contrast target, fill in the data form bubble representing the smallest contrast circle seen for each row (3%, 6%, 12%, 25%, 50%) for each of three positions. First, hold the contrast target at arms length just below the light source on the horizon and facing the light source (with glare in your eyes). Second, repeat this with your observing partner blocking the glare with a clipboard. Third, face away from the light source with it fully illuminating the target at arms length (so the light is coming over your shoulder and shining on the target.
- Next, face toward and look at the light source for 1 minute, then look away and protect your eyes from all light sources for 1 minute to prepare your eyes for the star count. Next, using the constellation Lyra star chart (area # l3), determine the dimmest star (highest number) you can see and record this number. Spend at least 1 minute and no more than 5 minutes doing this. This area of the sky is roughly 3x5 degrees and adjacent to the bright star Vega which is nearly overhead. You may find it easiest to lie on your back. You will probably need a dim red light to read the chart.
- Last, with your eyes still dark-adapted from the star count exercise, make observations and any notes on the subtle Zodiacal Light (http://en.wikipedia.orglwiki/Zodiacal_light) and Milky Way. You can make relative observations, such as "as compared to the 4 mile point, I can see many more dark pockets in the Cygnus area of the Milky Way."

Quantitative Data Gathering

These Sky Quality Meter-L quantitative measurements can be used to determine the distance at which illumination falls below the threshold of 0.1 millilux (even if the transect doesn't reach that far out). It can also be used to crudely estimate the total luminance of the light source. These calculations are accomplished with an Excel Spreadsheet, which will be provided later. The NPS can also post-calibrate the BLM SQM-L units to produce more accurate measurements.

- Set measurement locations at 4, 6, 8, 10, 12, and 14 statute miles from light source center. Small variances in these distances are fine. A minimum of three points are required.
- When first taking readings at a transect location, discard the first measurement as it is often spurious.
- You will take three readings pointed at three targets. When the data is reduced, only the median value will be used, but record all three on the datasheet. First, point the SQM-L directly overhead at the zenith and record the three readings. Second, point the SQM-L directly at the light source, holding it 6' above ground level. Third, point the SQM-L horizontally at a natural portion of the horizon. Do your best to match the same terrain being aimed at (mountain vs. playa vs. vegetation). This last measure will be subtracted from the light source measure to isolate the artificial light component.

C. 2011 protocol discussion.

Appendix B summarizes the 2011 Burning Man artificial light at night (ALAN) evaluation protocol, which was repeated as best possible for the 2017 event.

At the time that the more comprehensive 2017 ALAN protocol was proposed it was noted that the 2011 Protocol was dated and, in many ways, deficient as an objective, scientific measure of temporal changes due to the event itself. Western Research Company personnel indicated that these deficiencies were sufficiently great that it was agreed that little effort would be expended on evaluating the resultant observations. It is not the purpose of this report to provide a detailed critique of the shortcomings of the 2011 Protocol, but some key issues are identified here.

The 2011 Protocol can be broadly divided into two parts: 1) qualitative psycho-visual observations, and 2) quantitative photometric measurements. Both are discussed below.

Psycho-visual Observations

This part of the protocol involved recording responses to a series of contrast targets under differing light conditions (a function of distance from the light source), as well as subjective observations of the quality and character of the night sky. These are legitimate observations to make if set up properly. The prescribed protocol, however, yields nearly useless data.

The problem is at least four-fold: 1) there are too few observers, 2) there is no "calibration:" of the observers, 3) critical atmospheric and sky conditions are not adequately characterized, and 4) the observations are "snapshots" of very temporal and dynamic light environments.

In the first instance it should be noted that it is possible to calculate the number of observers needed to achieve defined levels of certainty in the observational data; the result typically requires 50 or more observers to obtain useful data. For the pairs of observers actually used, there is no "calibration" of visual acuity, age, experience working in low light levels, etc. Each of the observations is a strong function of local atmospheric and sky conditions, for which little useful characterization is provided. Finally, the observations consist of a few minutes of data collection at each of several sites spread over a period of several hours; in the meantime the source of the light can be shown to be undergoing significant variation.

All of these primary (and several secondary) factors render this part of the data collection of limited value. Careful examination of the data sets will show graphically how untrustworthy these results are.

Photometric Observations

A set of quantitative photometric measurements was made at each site with the intent that the sky and source brightness could be compared as seen from each site as well as from different epochs (in this case 2011 to 2017). This is a potentially more valuable metric than the small sample size psycho-visual observations, but this protocol is not as useful as it might have been.

The problem here is two-fold: 1) the data collected are too few to be very meaningful, and 2) the 2011 measurements were made at too few sites to achieve the goal of the protocol.

In the first instance it should be noted that sky brightness can change significantly during the course of a single night, and certainly between nights. This is true even between times of astronomical twilight and on moonless nights. To sample ALAN for a few seconds from different times of night on a single night is not very informative.

Second, to satisfy the purported goals of the 2011 Protocol, observing from three sites, as was done in 2011, does not provide enough data points to get a good picture of sky brightness as a function of distance from the source.

To get a sense of this, compare 2011 with more numerous 2017 SQM measurements as shown in the graphic below. Circles are 2011 measurements; and diamonds are 2017 data. The fit is to the 2017 data. In each instance there are six measurements per site, made over a period of a few minutes.

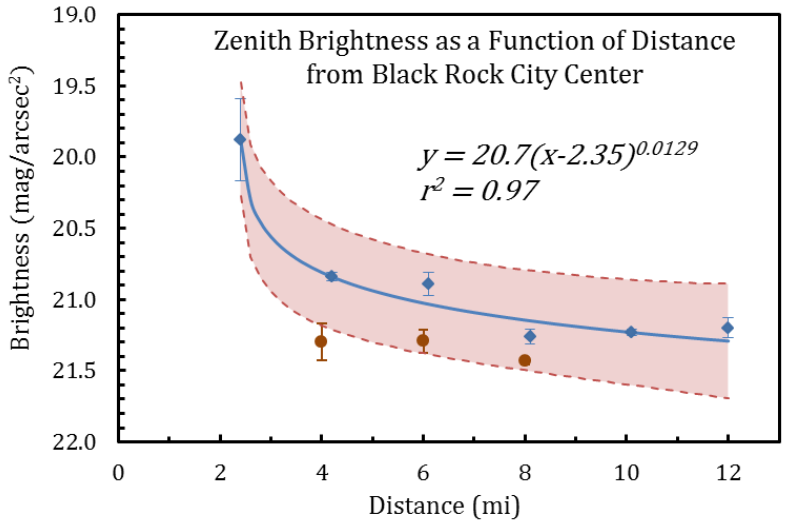

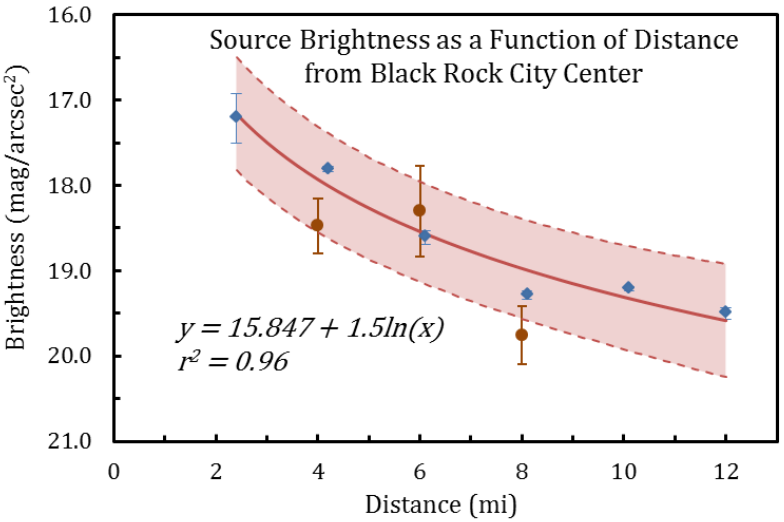

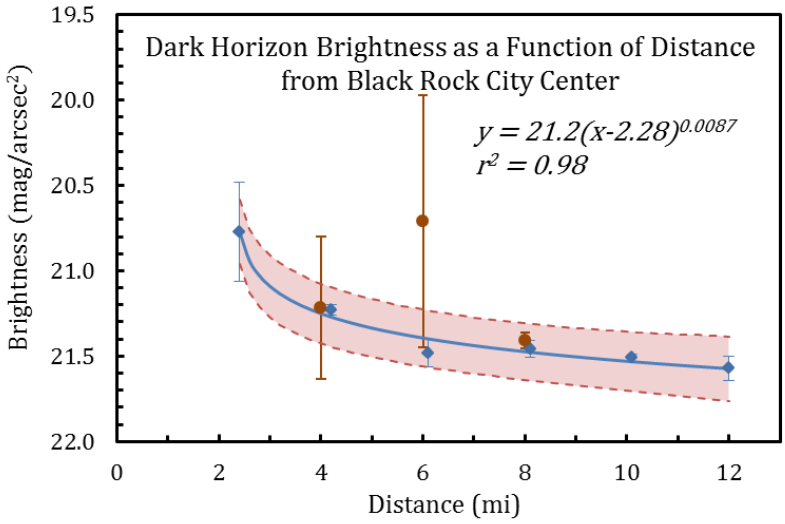

Summary

The 2011 Protocol as originally written is of little value. If it is to be used in the future it should be significantly modified.

In the meantime, technology of ALAN measurement has become more sophisticated and a better choice would be to restructure the ground-based protocol altogether.

D. Burning Man Event Dates.

The Burning Man event dates (Benson, Marnee (Associate Director of Government Affairs Burning Man), personal communication).

Gate Opening		Gate Closure	
Date	**Time**	**Date**	**Time**
Sunday August 27th, 2017	00:01	Tuesday September 5th, 2017	12:00
Sunday August 28th, 2016	00:01	Tuesday September 6th, 2016	12:00
Sunday, August 30, 2015	10:00	Tuesday, September 8th, 2015	12:00
Sunday, August 24th, 2014	17:00	Tuesday September 2nd, 2014	12:00
Sunday, August 25th, 2013	17:00	Tuesday September 3rd, 2013	12:00
Sunday, August 26th, 2012	17:00	Tuesday September 4th, 2012	12:00

E. Satellite observation nights.

Nights and times of satellite imagery obtained are listed. Image data was corrected for lunar illumination, normalized for zenith angle, or had a cloud index greater than 0.1 is indicated (Y, yes; N, no). The disqualified nights, not used in any analyses, are shaded in red.

Date	Time(UTC)	Lunar corrected	ZA normalized	Cloud Index >0.1
15-Aug-2012	09:37	N	N	Y
17-Aug-2012	09:01	N	N	N
20-Aug-2012	09:46	N	N	N
22-Aug-2012	09:05	N	N	N
23-Aug-2012	08:48	N	N	N
25-Aug-2012	09:49	N	N	Y
26-Aug-2012	09:32	N	N	Y
27-Aug-2012	09:14	Y	N	N
28-Aug-2012	08:51	Y	N	N
30-Aug-2012	09:59	Y	N	Y
31-Aug-2012	09:35	Y	N	Y
1-Sep-2012	09:18	Y	N	N
2-Sep-2012	09:00	Y	N	N
3-Sep-2012	08:43	N	N	N
13-Sep-2012	08:56	Y	N	Y
21-Aug-2013	10:22	Y	Y	Y
22-Aug-2013	10:04	Y	Y	N
23-Aug-2013	09:47	Y	Y	N
24-Aug-2013	09:29	Y	Y	N
25-Aug-2013	09:06	Y	Y	N
26-Aug-2013	08:49	Y	Y	N
27-Aug-2013	10:14	Y	Y	N
28-Aug-2013	09:50	Y	Y	Y
29-Aug-2013	09:33	Y	Y	Y
30-Aug-2013	09:15	Y	Y	N
31-Aug-2013	08:58	N	Y	N
1-Sep-2013	10:17	Y	Y	Y
2-Sep-2013	10:00	N	Y	N
3-Sep-2013	09:42	N	Y	Y
4-Sep-2013	09:19	N	Y	Y
21-Aug-2014	09:50	N	Y	Y
22-Aug-2014	09:27	N	Y	N
23-Aug-2014	09:09	N	Y	N

Date	Time(UTC)	Lunar corrected	ZA normalized	Cloud Index >0.1
24-Aug-2014	08:52	N	Y	N
25-Aug-2014	10:11	N	Y	Y
26-Aug-2014	09:54	N	Y	N
27-Aug-2014	09:36	N	Y	N
28-Aug-2014	09:19	N	Y	N
29-Aug-2014	08:55	N	Y	N
30-Aug-2014	10:20	N	Y	N
31-Aug-2014	10:03	N	Y	N
1-Sep-2014	09:40	N	Y	N
2-Sep-2014	09:22	N	Y	N
3-Sep-2014	09:05	N	Y	N
4-Sep-2014	08:47	N	Y	N
21-Aug-2015	09:01	Y	Y	N
22-Aug-2015	10:20	Y	Y	N
23-Aug-2015	10:03	Y	Y	N
24-Aug-2015	09:45	Y	Y	N
25-Aug-2015	09:22	Y	Y	N
26-Aug-2015	09:05	Y	Y	N
27-Aug-2015	10:30	Y	Y	N
28-Aug-2015	10:06	Y	Y	N
29-Aug-2015	09:49	Y	Y	Y
30-Aug-2015	09:31	Y	Y	N
31-Aug-2015	09:14	Y	Y	N
1-Sep-2015	08:51	Y	Y	N
2-Sep-2015	10:16	Y	Y	N
3-Sep-2015	09:58	Y	Y	N
4-Sep-2015	09:35	Y	Y	N
5-Sep-2015	11:00	Y	Y	N
5-Sep-2015	09:18	Y	Y	N
6-Sep-2015	09:00	Y	Y	N
7-Sep-2015	10:19	Y	Y	N
8-Sep-2015	10:02	Y	Y	N
9-Sep-2015	09:44	Y	Y	N
10-Sep-2015	09:27	Y	Y	Y
15-Sep-2015	09:30	Y	Y	Y
16-Sep-2015	10:50	Y	Y	Y
14-Jun-2016	09:10	N	Y	Y
15-Jun-2016	08:52	Y	Y	Y
17-Jun-2016	09:54	Y	Y	N
18-Jun-2016	09:36	Y	Y	N

Date	Time(UTC)	Lunar corrected	ZA normalized	Cloud Index >0.1
20-Jun-2016	08:56	Y	Y	N
22-Jun-2016	09:57	Y	Y	N
5-Jul-2016	09:18	N	Y	N
6-Jul-2016	08:54	N	Y	N
7-Jul-2016	08:37	N	Y	N
1-Aug-2016	10:48	N	Y	N
2-Aug-2016	10:31	N	Y	N
3-Aug-2016	10:13	N	Y	N
5-Aug-2016	09:33	N	Y	Y
7-Aug-2016	10:35	N	Y	N
8-Aug-2016	10:17	N	Y	Y
9-Aug-2016	10:00	N	Y	N
10-Aug-2016	09:42	N	Y	Y
12-Aug-2016	09:01	N	Y	N
13-Aug-2016	10:26	N	Y	N
15-Aug-2016	09:46	Y	Y	N
16-Aug-2016	09:28	Y	Y	N
17-Aug-2016	09:11	Y	Y	N
18-Aug-2016	08:47	Y	Y	Y
20-Aug-2016	09:55	Y	Y	N
21-Aug-2016	09:32	Y	Y	N
22-Aug-2016	09:14	Y	Y	Y
23-Aug-2016	08:57	Y	Y	N
24-Aug-2016	08:39	Y	Y	N
25-Aug-2016	09:58	Y	Y	N
26-Aug-2016	09:41	Y	Y	N
27-Aug-2016	09:23	Y	Y	Y
28-Aug-2016	09:00	N	Y	N
28-Aug-2016	10:43	Y	Y	N
29-Aug-2016	08:43	N	Y	N
29-Aug-2016	10:25	N	Y	N
30-Aug-2016	10:08	N	Y	Y
31-Aug-2016	09:44	N	Y	Y
1-Sep-2016	09:27	N	Y	N
2-Sep-2016	09:09	N	Y	N
2-Sep-2016	10:52	N	Y	Y
3-Sep-2016	08:52	N	Y	Y
3-Sep-2016	10:29	N	Y	N

Date	Time(UTC)	Lunar corrected	ZA normalized	Cloud Index >0.1
5-Sep-2016	09:54	N	Y	N
6-Sep-2016	09:36	N	Y	N
7-Sep-2016	09:13	N	Y	N
9-Sep-2016	10:20	N	Y	N
11-Sep-2016	09:40	N	Y	N
13-Sep-2016	09:05	Y	Y	Y
2-Oct-2016	09:48	N	Y	N
3-Oct-2016	09:30	N	Y	N
4-Oct-2016	09:07	N	Y	N
5-Oct-2016	08:49	N	Y	Y
1-Aug-2017	10:05	N	N	Y
2-Aug-2017	09:48	N	N	Y
6-Aug-2017	10:09	Y	N	Y
7-Aug-2017	09:51	Y	N	N
9-Aug-2017	09:16	Y	N	N
12-Aug-2017	10:01	Y	N	N
15-Aug-2017	09:02	Y	N	N
18-Aug-2017	09:47	N	N	N
19-Aug-2017	09:29	N	N	N
20-Aug-2017	09:06	N	N	N
21-Aug-2017	10:31	N	N	N
22-Aug-2017	10:13	N	N	Y
23-Aug-2017	09:50	N	N	N
24-Aug-2017	09:33	N	N	N
25-Aug-2017	09:15	N	N	N
25-Aug-2017	10:58	N	N	N
26-Aug-2017	08:58	N	N	N
26-Aug-2017	10:34	N	N	N
27-Aug-2017	10:17	N	N	Y
28-Aug-2017	09:59	N	N	N
29-Aug-2017	09:42	N	N	N
30-Aug-2017	09:19	N	N	Y
31-Aug-2017	09:01	N	N	N
31-Aug-2017	10:44	N	N	N
1-Sep-2017	10:26	N	N	Y
2-Sep-2017	10:03	N	N	Y
3-Sep-2017	09:45	Y	N	N
4-Sep-2017	09:28	Y	N	Y
5-Sep-2017	09:10	Y	N	Y
6-Sep-2017	10:30	Y	N	Y

Date	Time(UTC)	Lunar corrected	ZA normalized	Cloud Index >0.1
7-Sep-2017	10:12	Y	N	Y
8-Sep-2017	09:55	Y	N	Y
9-Sep-2017	09:32	Y	N	Y
10-Sep-2017	09:14	Y	N	N
11-Sep-2017	10:39	Y	N	N
12-Sep-2017	10:16	Y	N	Y

F. Ground-based log summary.

In this Appendix the ground-based log sheets are summarized. There were two observers, each completing six log sheets. The results are collapsed here to a summary of both observers' observations on a single log for each of the six sites. Only the subjective observations are included here; the quantitative SQM-L measurements are recorded and discussed elsewhere in this report.

Observed responses are indicated by a "+" or a "x" for the two observers. Compare the site numbers with Table 3.2 and Figure 3.5.

Experimental Night Lightscape Datasheet

Date: 8/27/17 Time: 8/28 0150 Transect: Approx Distance: 2.4 sm

Observer: Lat/Long: site 6

Nocturnal Scene:

Artificial Light
- ☒ Dominating landscape (like full moon)
- ☐ Strongly interfering w/ vision (quarter moon)
- ☐ Weakly interfering w/ vision (very thin crescent moon or Venus)
- ☐ Noticable but not interfering (like Jupiter or Sirius)
- ☐ Barely seen

Terrain illumination
- ☒ Texture seen easily
- ☐ Texture seen with difficulty
- ☐ Texture not seen
- ☒ Forms seen easily
- ☐ Forms seen with difficulty

Light Pollution domes
- ☐ Covers entire sky
- ☒ Reaches above 60°
- ☒ Reaches above 45°
- ☐ Reaches above 30°
- ☐ Reaches above 15°
- ☐ Just at horizon
- ☐ Not seen

Shadows
- ☒ Obvious LP shadows
- ☐ Weak LP shadows
- ☐ Very weak LP shadows
- ☐ LP shadows not seen
- ☒ Light colored ground
- ☒ Medium colored ground
- ☐ Dark colored ground

Visual Contrast:

Facing light source with Glare

3% ○○○ ○○○ ○○○
6% ○○○ ○○○ ○○○
12% ○○○ ○○○ ○○○
25% ○○○ ○○○ ○○○
50% ○○○ ○○○ ○○○

Smallest size print readable: n/a

Facing light source without Glare

3% ○○○ ○○○ ○○○
6% ○○○ ○○○ ○○○
12% ○○○ ○○○ ○○○
25% ○○○ ○○○ ○○○
50% ○○○ ○○○ ○○○

Smallest size print readable: n/a

Facing away from light source

3% ○○○ ○○○ ○○○
6% ○○○ ○○○ ○○○
12% ○○○ ○○○ ○○○
25% ○○○ ○○○ ○○○
50% ○○○ ○○○ ○○○

Smallest size print readable: n/a

Limiting Magnitude n/a (Area #13— Lyra—observe after one minutes exposed to glare and one minute of darkness)

Natural Features of the Night:

Milky Way (Cas to Sag)
- ☐ Intricate and veined
- ☐ Complex, defined edges
- ☐ Faint but continuous >90°
- ☐ Faint but continuous <90°
- ☐ Discontinuous
- ☐ Not seen

cloud

Zodiacal Light
- ☐ Entire Band
- ☐ Reaches above 60°
- ☐ Reaches above 45°
- ☐ Reaches above 30°
- ☐ Reaches above 15°
- ☐ Possibly seen at horizon
- ☒ Not seen

SQM-L Measurements: Serial # _____

Zenith (vertical)	Light Source (horizontal)	Dark Horizon (horizonal)

Experimental Night Lightscape Datasheet

Date: 8/27/17 Time: 8/28 0110 Transect: Approx Distance: 4.1 sm

Observer: Lat/Long: site 5

Nocturnal Scene:

Artificial Light
- ☒ Dominating landscape (like full moon)
- ☐ Strongly interfering w/ vision (quarter moon)
- ☐ Weakly interfering w/ vision (very thin crescent moon or Venus)
- ☐ Noticable but not interfering (like Jupiter or Sirius)
- ☐ Barely seen

Terrain illumination
- ☒ Texture seen easily
- ☐ Texture seen with difficulty
- ☐ Texture not seen
- ☒ Forms seen easily
- ☐ Forms seen with difficulty

Light Pollution domes
- ☐ Covers entire sky
- ☒ Reaches above 60°
- ☐ Reaches above 45°
- ☐ Reaches above 30°
- ☐ Reaches above 15°
- ☐ Just at horizon
- ☐ Not seen

Shadows
- ☒ Obvious LP shadows
- ☐ Weak LP shadows
- ☐ Very weak LP shadows
- ☐ LP shadows not seen

- ☐ Light colored ground
- ☒ Medium colored ground
- ☐ Dark colored ground

Visual Contrast:

Facing light source with Glare

3% ○○○ ○○○ ○○○
6% ○○○ ○○○ ○○○
12% ○○○ ○○○ ○○○
25% ○○○ ○○○ ○○○
50% ○○○ ○○○ ○○○

Smallest size print readable: n/a

Facing light source without Glare

3% ○○○ ○○○ ○○○
6% ○○○ ○○○ ○○○
12% ○○○ ○○○ ○○○
25% ○○○ ○○○ ○○○
50% ○○○ ○○○ ○○○

Smallest size print readable: n/a

Facing away from light source

3% ○○○ ○○○ ○○○
6% ○○○ ○○○ ○○○
12% ○○○ ○○○ ○○○
25% ○○○ ○○○ ○○○
50% ○○○ ○○○ ○○○

Smallest size print readable: n/a

Limiting Magnitude 4.3 (Area #13— Lyra—observe after one minutes exposed to glare and one minute of darkness)

Natural Features of the Night:

Milky Way (Cas to Sag)
- ☐ Intricate and veined
- ☐ Complex, defined edges
- ☒ Faint but continuous >90°
- ☐ Faint but continuous <90°
- ☐ Discontinuous
- ☐ Not seen

Zodiacal Light
- ☐ Entire Band
- ☐ Reaches above 60°
- ☐ Reaches above 45°
- ☐ Reaches above 30°
- ☐ Reaches above 15°
- ☐ Possibly seen at horizon
- ☒ Not seen

SQM-L Measurements: Serial # _____

Zenith (vertical)	Light Source (horizontal)	Dark Horizon (horizonal)

Experimental Night Lightscape Datasheet

Date: 8/27/17 Time: 0030 8/28 Transect: Approx Distance: 6.1 sm

Observer: Lat/Long: Site 4

Nocturnal Scene:

Artificial Light
- ☒ Dominating landscape (like full moon)
- ☐ Strongly interfering w/ vision (quarter moon)
- ☐ Weakly interfering w/ vision (very thin crescent moon or Venus)
- ☐ Noticable but not interfering (like Jupiter or Sirius)
- ☐ Barely seen

Terrain illumination
- ☒ Texture seen easily
- ☐ Texture seen with difficulty
- ☐ Texture not seen

- ☒ Forms seen easily
- ☐ Forms seen with difficulty

Light Pollution domes
- ☐ Covers entire sky
- ☒ Reaches above 60°
- ☐ Reaches above 45°
- ☐ Reaches above 30°
- ☐ Reaches above 15°
- ☐ Just at horizon
- ☐ Not seen

Shadows
- ☐ Obvious LP shadows
- ☒ Weak LP shadows
- ☒ Very weak LP shadows
- ☐ LP shadows not seen

- ☒ Light colored ground
- ☒ Medium colored ground
- ☐ Dark colored ground

Visual Contrast:

Facing light source with Glare

3% ☒ ○ ○○○ ○○○ Smallest size print readable
6% ○○○ ☒ ○ ○○○
12% ○○○ ☒ ☒ ○○○ n/a
25% ○○○ ☒ ☒ ○○○
50% ○○○ ☒ ☒ ○○○

Facing light source without Glare

3% ☒ ○ ○○○ ○○○ Smallest size print readable
6% ○○○ ☒ ○ ○○○
12% ○○○ ☒ ☒ ○○○ n/a
25% ○○○ ☒ ☒ ○○○
50% ○○○ ☒ ☒ ○○○

Facing away from light source

3% ○ ☒ ○ ○○○ ○○○ Smallest size print readable
6% ○○○ ☒ ☒ ○○○
12% ○○○ ☒ ☒ ○○○ n/a
25% ○○○ ☒ ☒ ○○○
50% ○○○ ☒ ☒ ○○○

Limiting Magnitude 4.3 (Area #13— Lyra—observe after one minutes exposed to glare and one minute of darkness)

Natural Features of the Night:

Milky Way (Cas to Sag)
- ☐ Intricate and veined
- ☒ Complex, defined edges
- ☐ Faint but continuous >90°
- ☐ Faint but continuous <90°
- ☐ Discontinuous
- ☐ Not seen

Zodiacal Light
- ☐ Entire Band
- ☐ Reaches above 60°
- ☐ Reaches above 45°
- ☐ Reaches above 30°
- ☐ Reaches above 15°
- ☐ Possibly seen at horizon
- ☒ Not seen

SQM-L Measurements: Serial # _____

Zenith (vertical)	Light Source (horizontal)	Dark Horizon (horizonal)

Experimental Night Lightscape Datasheet

Date: 8/27/17 Time: 2400M Transect: Approx Distance: 8.1 SM

Observer: Lat/Long: site, 3

Nocturnal Scene:

Artificial Light
- [x] Dominating landscape (like full moon)
- [ ] Strongly interfering w/ vision (quarter moon)
- [ ] Weakly interfering w/ vision (very thin crescent moon or Venus)
- [ ] Noticable but not interfering (like Jupiter or Sirius)
- [ ] Barely seen

Terrain illumination
- [x] Texture seen easily
- [ ] Texture seen with difficulty
- [ ] Texture not seen
- [x] Forms seen easily
- [ ] Forms seen with difficulty

Light Pollution domes
- [ ] Covers entire sky
- [x] Reaches above 60°
- [ ] Reaches above 45°
- [ ] Reaches above 30°
- [ ] Reaches above 15°
- [ ] Just at horizon
- [ ] Not seen

Shadows
- [ ] Obvious LP shadows
- [ ] Weak LP shadows
- [x] Very weak LP shadows
- [ ] LP shadows not seen

- [x] Light colored ground
- [x] Medium colored ground
- [ ] Dark colored ground

Visual Contrast:

Facing light source with Glare

3% X OOO OOO OOO
6% OOO X OOO OOO
12% OOO X OOO OOO
25% OOO X OOO
50% OOO X OOO

Smallest size print readable: n/a

Facing light source without Glare

3% X OOO OOO OOO
6% OOO X OOO OOO
12% OOO X OOO OOO
25% OOO X OOO
50% OOO X OOO

Smallest size print readable: n/a

Facing away from light source

3% X OOO OOO
6% OOO X OOO
12% OOO X OOO
25% OOO X OOO
50% OOO X OOO

Smallest size print readable: n/a

Limiting Magnitude 5.0 - 5.4 (Area #13— Lyra—observe after one minutes exposed to glare and one minute of darkness)

Natural Features of the Night:

Milky Way (Cas to Sag)
- [ ] Intricate and veined
- [x] Complex, defined edges
- [ ] Faint but continuous >90°
- [ ] Faint but continuous <90°
- [ ] Discontinuous
- [ ] Not seen

Zodiacal Light
- [ ] Entire Band
- [ ] Reaches above 60°
- [ ] Reaches above 45°
- [ ] Reaches above 30°
- [ ] Reaches above 15°
- [ ] Possibly seen at horizon
- [x] Not seen

SQM-L Measurements: Serial # _____

Zenith (vertical)	Light Source (horizontal)	Dark Horizon (horizonal)

Experimental Night Lightscape Datasheet

Date: 8/27/17 Time: 1130 PM Transect: Approx Distance: 10.1 sm

Observer: Lat/Long: Site 2

Nocturnal Scene:

Artificial Light
- ☒ Dominating landscape (like full moon)
- ☐ Strongly interfering w/ vision (quarter moon)
- ☐ Weakly interfering w/ vision (very thin crescent moon or Venus)
- ☐ Noticable but not interfering (like Jupiter or Sirius)
- ☐ Barely seen

Terrain illumination
- ☒ Texture seen easily
- ☐ Texture seen with difficulty
- ☐ Texture not seen
- ☒ Forms seen easily
- ☐ Forms seen with difficulty

Light Pollution domes
- ☐ Covers entire sky
- ☒ Reaches above 60°
- ☐ Reaches above 45°
- ☐ Reaches above 30°
- ☐ Reaches above 15°
- ☐ Just at horizon
- ☐ Not seen

Shadows
- ☐ Obvious LP shadows
- ☐ Weak LP shadows
- ☒ Very weak LP shadows
- ☐ LP shadows not seen
- ☐ Light colored ground
- ☒ Medium colored ground
- ☐ Dark colored ground

Visual Contrast:

Facing light source with Glare

3% ○○○ ○○○ ○○○
6% ○○○ ○○○ ○○○
12% ○○○ ○○○ ○○○
25% ○○○ ○○○ ○○○
50% ○○○ ○○○ ○○○

Smallest size print readable: n/a

Facing light source without Glare

3% ○○○ ○○○ ○○○
6% ○○○ ○○○ ○○○
12% ○○○ ○○○ ○○○
25% ○○○ ○○○ ○○○
50% ○○○ ○○○ ○○○

Smallest size print readable: n/a

Facing away from light source

3% ○○○ ○○○ ○○○
6% ○○○ ○○○ ○○○
12% ○○○ ○○○ ○○○
25% ○○○ ○○○ ○○○
50% ○○○ ○○○ ○○○

Smallest size print readable: n/a

Limiting Magnitude 4-5 (Area #13— Lyra—observe after one minutes exposed to glare and one minute of darkness)

Natural Features of the Night:

Milky Way (Cas to Sag)
- ☐ Intricate and veined
- ☐ Complex, defined edges
- ☐ Faint but continuous >90°
- ☐ Faint but continuous <90°
- ☐ Discontinuous
- ☐ Not seen

cloud

Zodiacal Light
- ☐ Entire Band
- ☐ Reaches above 60°
- ☐ Reaches above 45°
- ☐ Reaches above 30°
- ☐ Reaches above 15°
- ☐ Possibly seen at horizon
- ☐ Not seen

cloud

SQM-L Measurements: Serial # _____

Zenith (vertical)	Light Source (horizontal)	Dark Horizon (horizonal)

Experimental Night Lightscape Datasheet

Date: 8/27/17 Time: 1100 PM Transect: Approx Distance: 12 sm

Observer: Lat/Long: site 1

Nocturnal Scene:

Artificial Light
- ☒ Dominating landscape (like full moon)
- ☒ Strongly interfering w/ vision (quarter moon)
- ☐ Weakly interfering w/ vision (very thin crescent moon or Venus)
- ☐ Noticable but not interfering (like Jupiter or Sirius)
- ☐ Barely seen

Terrain illumination
- ☒ Texture seen easily
- ☒ Texture seen with difficulty
- ☐ Texture not seen
- ☒ Forms seen easily
- ☐ Forms seen with difficulty

Light Pollution domes
- ☐ Covers entire sky
- ☐ Reaches above 60°
- ☐ Reaches above 45°
- ☒ Reaches above 30°
- ☐ Reaches above 15°
- ☐ Just at horizon
- ☐ Not seen

Shadows
- ☐ Obvious LP shadows
- ☐ Weak LP shadows
- ☐ Very weak LP shadows
- ☒ LP shadows not seen

- ☒ Light colored ground
- ☒ Medium colored ground
- ☐ Dark colored ground

Visual Contrast:

Facing light source with Glare

3% ○○○ ○○○ ○○○
6% ○○✱ ○○○ ○○○
12% ○○○ ✱✱ ○○○
25% ○○○ ✱✱ ○○○
50% ○○○ ✱✱ ○○○

Smallest size print readable: n/a

Facing light source without Glare

3% ✱○○ ○○○ ○○○
6% ○○○ ✱✱ ○○○
12% ○○○ ✱✱ ○○○
25% ○○○ ✱✱ ○○○
50% ○○○ ✱✱ ○○○

Smallest size print readable: n/a

Facing away from light source

3% ✱✱○ ○○○ ○○○
6% ○○○ ✱✱ ○○○
12% ○○○ ✱✱ ○○○
25% ○○○ ✱✱ ○○○
50% ○○○ ✱✱ ○○○

Smallest size print readable: n/a

Limiting Magnitude n/a (Area #13— Lyra—observe after one minutes exposed to glare and one minute of darkness)

Natural Features of the Night:

Milky Way (Cas to Sag)
- ☐ Intricate and veined
- ☐ Complex, defined edges
- ☐ Faint but continuous >90°
- ☐ Faint but continuous <90°
- ☐ Discontinuous
- ☐ Not seen

cloud

Zodiacal Light
- ☐ Entire Band
- ☐ Reaches above 60°
- ☐ Reaches above 45°
- ☐ Reaches above 30°
- ☐ Reaches above 15°
- ☐ Possibly seen at horizon
- ☐ Not seen

cloud

SQM-L Measurements: Serial # _____

Zenith (vertical)	Light Source (horizontal)	Dark Horizon (horizonal)